CENTRORADIALIS Interacts with *FLOWERING LOCUS T*-Like Genes to Control Floret Development and Grain Number[1][OPEN]

Xiaojing Bi,[a,b] Wilma van Esse,[c] Mohamed Aman Mulki,[a] Gwendolyn Kirschner,[d,e] Jinshun Zhong,[a,b] Rüdiger Simon,[d,e] and Maria von Korff[a,b,d,2,3]

[a]Max Planck Institute for Plant Breeding Research, D-50829 Cologne, Germany
[b]Institute of Plant Genetics, Heinrich-Heine-University, 40225 Düsseldorf, Germany
[c]Laboratory of Molecular Biology, Wageningen University and Research, Droevendaalsesteeg 1, 6708 PB Wageningen, the Netherlands
[d]Cluster of Excellence on Plant Sciences "SMART Plants for Tomorrow's Needs" 40225 Düsseldorf, Germany
[e]Institute for Developmental Genetics, Heinrich-Heine-University, 40225 Düsseldorf, Germany

ORCID IDs: 0000-0003-2240-1246 (X.B.); 0000-0003-3511-537X (M.A.M.); 0000-0001-7086-5470 (J.Z.); 0000-0002-6816-586X (M.v.K.).

CENTRORADIALIS (CEN) is a key regulator of flowering time and inflorescence architecture in plants. Natural variation in the barley (*Hordeum vulgare*) homolog HvCEN is important for agricultural range expansion of barley cultivation, but its effects on shoot and spike architecture and consequently yield have not yet been characterized. Here, we evaluated 23 independent *hvcen,* also termed *mat-c,* mutants to determine the pleiotropic effects of HvCEN on developmental timing and shoot and spike morphologies of barley under outdoor and controlled conditions. All *hvcen* mutants flowered early and showed a reduction in spikelet number per spike, tiller number, and yield in the outdoor experiments. Mutations in *hvcen* accelerated spikelet initiation and reduced axillary bud number in a photoperiod-independent manner but promoted floret development only under long days (LDs). The analysis of a *flowering locus t3* (*hvft3*) *hvcen* double mutant showed that HvCEN interacts with HvFT3 to control spikelet initiation. Furthermore, *early flowering3* (*hvelf3*) *hvcen* double mutants with high *HvFT1* expression levels under short days suggested that HvCEN interacts with HvFT1 to repress floral development. Global transcriptome profiling in developing shoot apices and inflorescences of mutant and wild-type plants revealed that HvCEN controlled transcripts involved in chromatin remodeling activities, cytokinin and cell cycle regulation and cellular respiration under LDs and short days, whereas HvCEN affected floral homeotic genes only under LDs. Understanding the stage and organ-specific functions of HvCEN and downstream molecular networks will allow the manipulation of different shoot and spike traits and thereby yield.

Shoot architecture is a major determinant of grain yield and therefore a primary target for crop improvement. Shoot architecture is largely defined by branching (tillering) patterns, plant height, leaf shape and arrangement, and inflorescence morphologies. These traits are controlled by the combined activities of the shoot apical meristem (SAM) and the axillary meristems (AXMs; Nakagawa et al., 2002; Teichmann and Muhr, 2015). A vegetative SAM gives rise to leaves and AXMs that form in the leaf axils (Turnbull, 2005). As plants transition from vegetative to reproductive growth, the SAM forms an inflorescence, flowers, and eventually seeds. Grasses exhibit a striking diversity in their inflorescence architectures that is determined by meristem initiation and determinacy decisions, the acquisition of spikelet meristem identity, and the determinacy of the spikelet meristem (Bommert and Whipple, 2018). The spikes of barley (*Hordeum vulgare*) display a raceme-like branchless shape and consist of triple spikelets produced on two opposite sides along the main axis (rachis). Although the barley inflorescence is indeterminate, the barley spikelet is determinate as a defined number of florets is produced, a maximum of a single floret and grain, per spikelet.

[1]This work was supported by the Deutsche Forschungsgemeinschaft (DFG) (German Research Foundation) under Germany's Excellence Strategy – EXC 2048/1 – 390686111; the Priority Programme (SPP1530 Flowering time control-from natural variation to crop improvement) and the Max-Planck-Gesellschaft (Max Planck Society); and a Chinese Scholarship Council fellowship (to X.B.).

[2]Author for contact: maria.korff.schmising@hhu.de.
[3]Senior author.

The author responsible for distribution of materials integral to the findings presented in this article in accordance with the policy described in the Instructions for Authors (www.plantphysiol.org) is: Maria von Korff (maria.korff.schmising@hhu.de).

X.B., W.v.E., M.A.M., and M.v.K. designed the experiments; X.B. carried out the experiments and analyzed the data; G.K. and R.S. conducted the in situ RNA hybridization; J.Z. contributed to the bioinformatic analyses; X.B. and M.v.K. wrote the manuscript; W.v.E., J.Z., R.S., and M.v.K. edited the manuscript; M.v.K. conceived the original research project.

[OPEN]Articles can be viewed without a subscription.
www.plantphysiol.org/cgi/doi/10.1104/pp.18.01454

The triple spikelet meristem of barley consists of one central spikelet meristem and two lateral spikelet meristems. Most studies on barley spike architecture have focused on the genetic basis of two-rowed versus six-rowed spikes, which is determined by differential development of the lateral spikelets (Komatsuda et al., 2007; Ramsay et al., 2011; Koppolu et al., 2013; Bull et al., 2017; van Esse et al., 2017; Youssef et al., 2017). However, recent studies have shown that spike architecture is also affected by genetic factors controlling the timing of preanthesis development in barley and wheat (*Triticum aestivum*). The flowering time regulators PHOTOPERIOD1 (PPD-H1) and its downstream target FLOWERING LOCUS T1 (FT1), homolog of Arabidopsis (*Arabidopsis thaliana*) FT, affect the number of spikelets produced on the main inflorescence in barley and wheat, likely by affecting the rate and duration of spikelet initiation (Boden et al., 2015; Digel et al., 2015). *FT*-like genes belong to phosphatidylethanolamine-binding proteins, whose homolog in humans (*Homo sapiens*) was characterized as a *Raf* kinase inhibitor protein, mediating the rapidly accelerated fibrosarcoma (RAF)/mitogen-activated protein kinase kinase (MEK)/extracellular signal-regulated kinases (ERK) signal transduction pathway (Bradley et al., 1996, 1997; Ohshima et al., 1997; Kardailsky et al., 1999; Kobayashi et al., 1999; Yeung et al., 1999). In plants, the phosphatidylethanolamine-binding proteins family comprises proteins with antagonistic effects on development as they either promote or inhibit floral transition. *FT*-like genes generally induce flowering while CENTRORADIALIS (CEN), first described in Garden Snapdragon (*Antirrhinum mayus*), represses the initiation of floral meristems (Bradley et al., 1996; Danilevskaya et al., 2008; Komiya et al., 2008; Turck et al., 2008; Digel et al., 2015; Kaneko-Suzuki et al., 2018). In Arabidopsis and rice (*Oryza sativa*), *FT* is expressed in the leaf vascular tissue and the FT protein is transported through the phloem to the SAM (Corbesier et al., 2007; Tamaki et al., 2007). In rice, the FT homolog HEADING DATE 3a (Hd3a) forms a florigen-activating complex with 14-3-3 proteins and FLOWERING LOCUS D (FD) homolog OsFD1 to activate the expression of meristem identity genes (Taoka et al., 2011). By contrast, TERMINAL FLOWER1 (TFL1), the Arabidopsis homolog of CEN, functions as a hypothetical competitor of FT in binding to FD and 14-3-3 proteins in the shoot apex, thereby preventing the induction of flowering (Abe et al., 2005; Wigge et al., 2005; Ahn et al., 2006; Hanano and Goto, 2011; McGarry and Ayre, 2012; Kaneko-Suzuki et al., 2018). An acceleration in flowering time and the formation of a terminal flower are observed in both *tfl1* mutants and plants overexpressing *FT* in Arabidopsis (Bradley et al., 1997; Kardailsky et al., 1999; Kobayashi et al., 1999). The function of TFL1 homologs in controlling flowering time and inflorescence architecture are conserved to some extent between grasses and eudicots. For example, the Antirrhinum TFL1 homolog CENTRORADIALIS controls the determinacy of the inflorescence with no effects on flowering time (Bradley et al., 1996), whereas LpTFL1 in ryegrass (*Lolium perenne*) represses flowering and controls AXM identity (Jensen et al., 2001). RICE CENTRORADIALIS (RCN1 and RCN2), rice homologs of TFL1, delay flowering and alter the panicle architecture (Nakagawa et al., 2002). Likewise, ectopic expression of the RCN1-CORN CENTRORADIALIS/TFL1-like protein *ZCN2*, *ZCN4*, *ZCN5* in maize (*Zea mays*) leads to late flowering and a bushy tassel with denser spikelets (Danilevskaya et al., 2010).

HvCEN, the barley homolog of Antirrhinum CEN and Arabidopsis TFL1, contributed to the expansion of barley cultivation into diverse habitats (Comadran et al., 2012). A natural Pro-135Ala substitution in HvCEN has been selected in spring barley cultivars and prolongs vegetative growth, while *hvcen* mutations lead to early flowering under natural long-day (LD) conditions (Comadran et al., 2012). The authors also show that induced *hvcen* mutants, originally designated as *maturity-c* (*mat-c*) mutants, flowered a few days earlier under natural LD conditions (Druka et al., 2011; Comadran et al., 2012; Lundqvist, 2014). However, the effects of HvCEN on shoot and inflorescence architecture and its interaction with *FT*-like genes have not been characterized so far.

Barley has six different FT-like homologs, of which only HvFT1 and HvFT3 have been functionally characterized (Schmitz et al., 2000; Yan et al., 2006; Hemming et al., 2008; Sasani et al., 2009; Casao et al., 2011; Chen and Dubcovsky, 2012; Halliwell et al., 2016). Elevated *HvFT1* expression in leaves is correlated with a strong acceleration of floral development, whereas HvFT3 only induces spikelet initiation without effects on later floret development (Digel et al., 2015; Mulki et al., 2018). In this study, we analyzed a large collection of independent *hvcen* mutants to (1) identify pleiotropic effects of HvCEN on developmental timing and shoot and spike morphology, (2) determine transcriptional targets of HvCEN in the developing SAM under different photoperiods, and (3) investigate the genetic interactions between *HvCEN* and the *FT*-like genes *HvFT1* and *HvFT3*.

We demonstrate that HvCEN has pleiotropic effects on several shoot traits, as it delays reproductive development and flowering, promotes axillary bud initiation/tillering, and increases the number of spikelet primordia and plant height. Mutations in HvCEN shortened the vegetative phase under both LDs and short days (SDs) but accelerated inflorescence development only under LDs. These photoperiod-specific effects of HvCEN were likely dependent on antagonistic interactions with different HvFT-like proteins during development. Global transcriptome analysis in developing SAMs suggested that spikelet initiation, as promoted by mutations in *hvcen*, coincided with a strong reprogramming of transcriptional networks, the induction of cell proliferation, and changes in the energy metabolism under SDs and LDs. The subsequent rapid floral development in the *hvcen* mutant

was linked to the LD-specific up-regulation of floral homeotic genes.

RESULTS

HvCEN Controls Shoot and Spike Architecture in Barley

To characterize the effects of different HvCEN mutations on shoot development, we analyzed flowering time, grains per spike, plant height, tiller number, and different seed parameters in 23 allelic *hvcen* mutants in six different spring barley backgrounds under outdoor conditions (Fig. 1; Supplemental Table S1). All the *hvcen* mutants flowered significantly earlier and produced fewer grains per main spike than the respective wild-type genotypes (Fig. 1, A and B). In addition, all *hvcen* mutants, except for *mat-c.19* and *mat-c.913*, produced fewer tillers at flowering time compared with the corresponding parental genotypes (Fig. 1C). Likewise, plant height of most *hvcen* mutants, excluding *mat-c.19*, *mat-c.32*, *mat-c.93* in the Bonus background and all mutants in the Frida background, was reduced compared with the respective wild-type genotypes (Fig. 1D). Seed traits, including length, width, area, and thousand kernel weight (TKW), were not significantly different between all mutants versus wild-type plants (Supplemental Fig. S1).

We calculated the degree of amino acid conservation across taxa for individual mutations. The analysis revealed that all single amino acid substitutions are located in conserved positions within the protein (Supplemental Table S2). The mutations were positioned in the potential ligand-binding pocket (*mat-c.913*, *mat-c.93*, *mat-c.32*, *mat-c.907*, *mat-c.1115*), the 14-3-3 protein interaction site (*mat-c.943*, *mat-c.745*), and the external loop (*mat-c.400*; Supplemental Fig. S2; Ahn et al., 2006; Ho and Weigel, 2014). The external loop has been

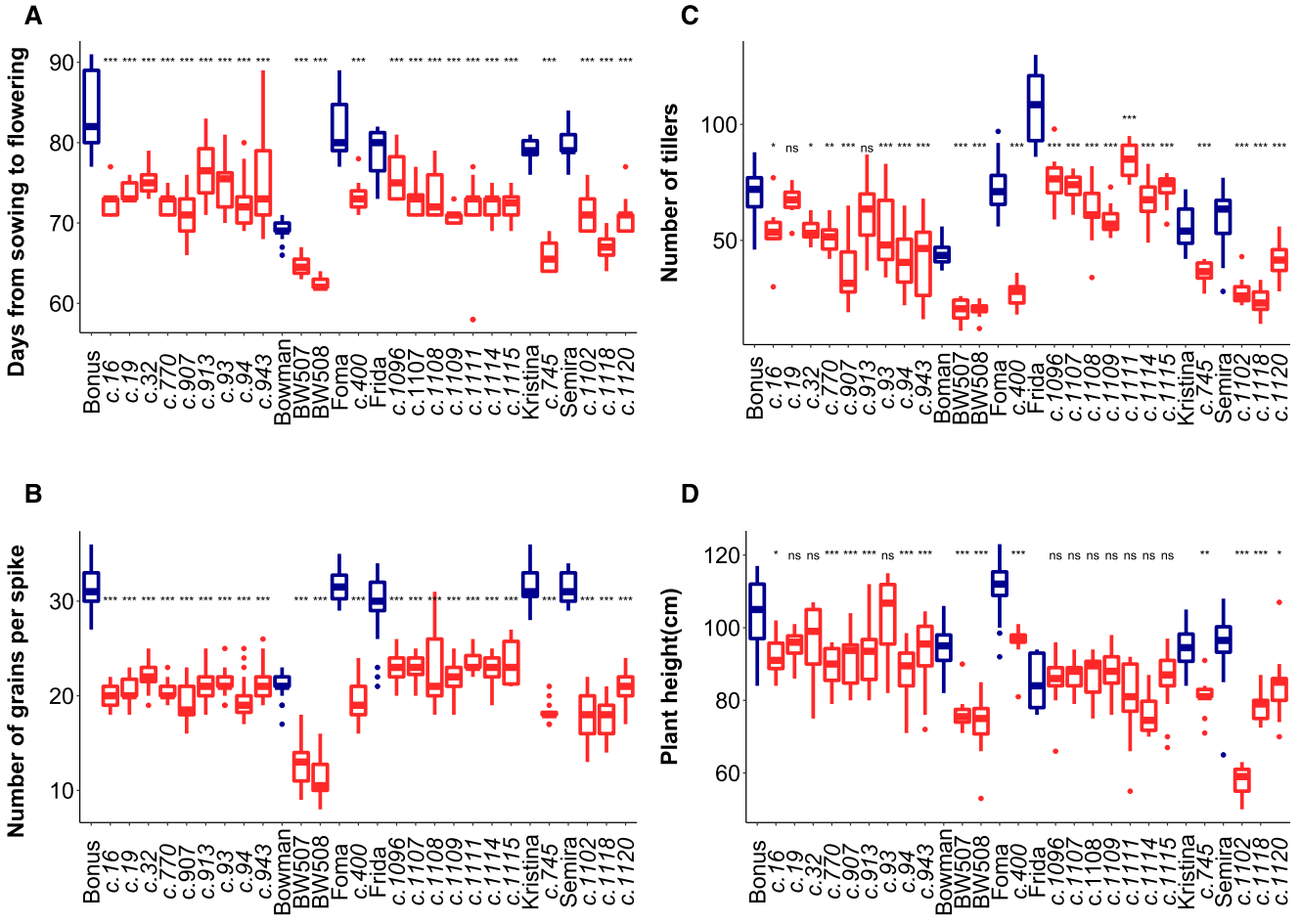

Figure 1. Phenotypes of *hvcen* (*mat-c*) mutants trialed under outdoor conditions over 2 consecutive years. Mutants (red) in six different genetic backgrounds are shown next to their respective parental lines (blue; Supplemental Table S1). Various traits including flowering time (A), grain number per main spike (B), number of tillers at flowering time (C), and plant height (D) were measured over years. Flowering time was scored as time from sowing to heading when the awn of the main spike emerged from the flag leaf. The line within each box denotes the median. The sample size per genotype is given in Supplemental Table S1. Error bars: SD. Significant differences between the mutants and their wild-type parents were calculated by a one-way ANOVA using a Tukey honestly significant difference as a post hoc test, $***P < 0.001$, $**P < 0.01$, $*P < 0.05$. ns, Not significant.

shown to represent the most substantial differences between FT and TFL1 and is critical for FT versus TFL1 activity in vivo (Ahn et al., 2006). The binding pocket has previously been suggested to play an important role in binding to phosphorylated interacting partners (Ahn et al., 2006; Ho and Weigel, 2014), whereas the 14-3-3 protein interaction site is important for the formation of the flowering activation complex (Taoka et al., 2011). All analyzed mutants showed a significant difference in most of the scored developmental traits, suggesting that these all altered the function of the protein.

To further illustrate the effects of HvCEN on reproductive development, we focused on the development of primary shoots of three selected *hvcen* mutants (*mat-c.907*, *mat-c.94*, *and mat-c.943*) and cv Bonus under different photoperiods. We also compared the timing of spikelet initiation and inflorescence development between the *hvcen* mutants and the wild-type parent Bonus (Fig. 2). The *hvcen* mutants initiated spikelet primordia (W2.0) significantly earlier under both LDs and SDs compared with the wild-type cv Bonus (Fig. 3, A and B). However, *hvcen* mutants exhibited photoperiod-specific patterns of growth and floret development. Particularly under LDs, floret development was greatly accelerated in *hvcen* mutants starting from the stamen primordium stage (W3.5; Fig. 3A). Consequently, the *hvcen* mutant plants flowered (W9.0-10.0) about 18 d earlier than Bonus under LDs (Fig. 3A). In contrast, floret development under SDs did not proceed beyond the stages W4.05.5 in the mutants and the stagesW3.5-W4.5 in Bonus (Figs. 2B and 3B).

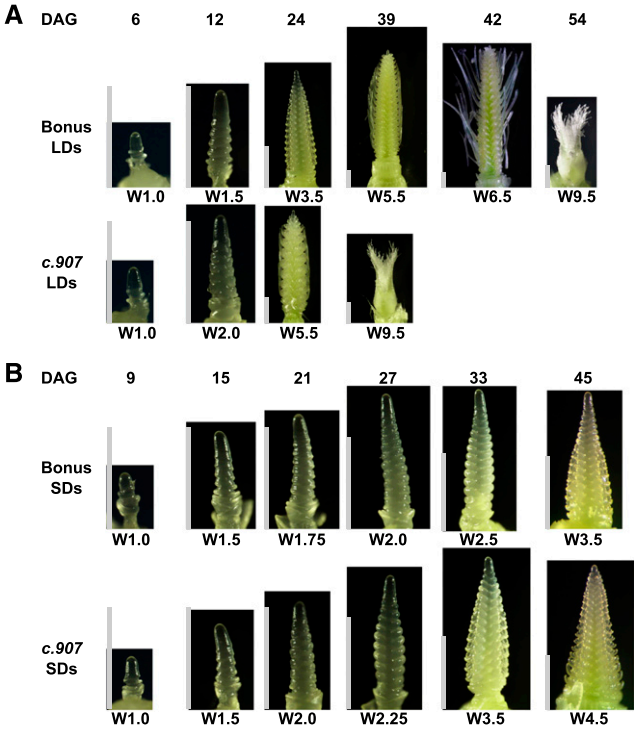

Figure 2. Representative shoot apices of the *hvcen* mutant and the wild type. Apices were scored under LD (A) and SD (B) conditions. Under SDs, the MSA did not develop beyond the stages W3.5 and W4.5 in the mutant and Bonus, respectively. DAG, days after germination; W, Waddington stage. White bar = 1 mm.

Because *hvcen* mutants displayed a reduction in grain number per main spike (Fig. 1B), we also evaluated the number of spikelet primordia initiated on the main shoot spike during development. Under LDs, the number of initiated spikelet primordia reached its maximal level at different developmental stages, in the mutant at W4.0 with 24.40 ± 1.58 spikelet primordia and in the wild type at W5.0 with 40.00 ± 0.76 primordia (Fig. 3C). Although the mutants developed fewer spikelet primordia, we did not observe the formation of a terminal spikelet as has been described for the Arabidopsis *tfl1* mutant and is typical for the determinate wheat inflorescence (Supplemental Fig. S3). Under SDs, the reduction in the number of spikelet primordia of *hvcen* mutants was only apparent before the lemma primordium stage (W3.0), and no differences were observed between the mutants and wild type after this stage (Fig. 3D). Furthermore, *hvcen* mutants produced fewer and shorter leaves on the main shoot (Supplemental Fig. S4) and exhibited a reduced number of axillary buds under both LDs and SDs (Fig. 3, E and F). No significant differences in leaf width were observed in the mutants compared with wild type except for *mat-c.943* with wider leaves under LDs (Supplemental Fig. S4).

Taken together, mutations in the three *hvcen (mat-c)* mutants accelerated the initiation of spikelet primordia under both LDs and SDs, whereas floret development of the mutants was only accelerated under LDs. Moreover, *hvcen* mutants exhibited a reduced number of spikelet primordia on the main shoot apex (MSA). Finally, HvCEN affected the total number of leaves and leaf size on the main culm and tiller number.

HvCEN Interacts with HvFT1 and HvFT3 to Control Reproductive Development under LDs and SDs

The HvCEN homolog TFL1 acts antagonistically to FT in the meristem, and the relative abundance of FT and TFL1 proteins controls floral development and shoot architecture in Arabidopsis and other crop plants (McGarry and Ayre, 2012; Kaneko-Suzuki et al., 2018). Therefore, we tested if and how the effects of HvCEN on development are dependent on the function of *FT*-like genes in barley. Barley has several *FT*-like genes (Halliwell et al., 2016); however, only *HvFT1* and *HvFT3* have been functionally analyzed and integrated into flowering pathways. *HvFT1* is only transcribed under LDs, and its protein promotes spikelet initiation and floret development (Yan et al., 2006; Digel et al., 2015). In contrast, *HvFT3* is expressed under SDs and LDs and specifically accelerates the timing of spikelet initiation but has no effects on floret development (Mulki et al., 2018). To test whether the effects of HvCEN on spikelet initiation are dependent on HvFT3,

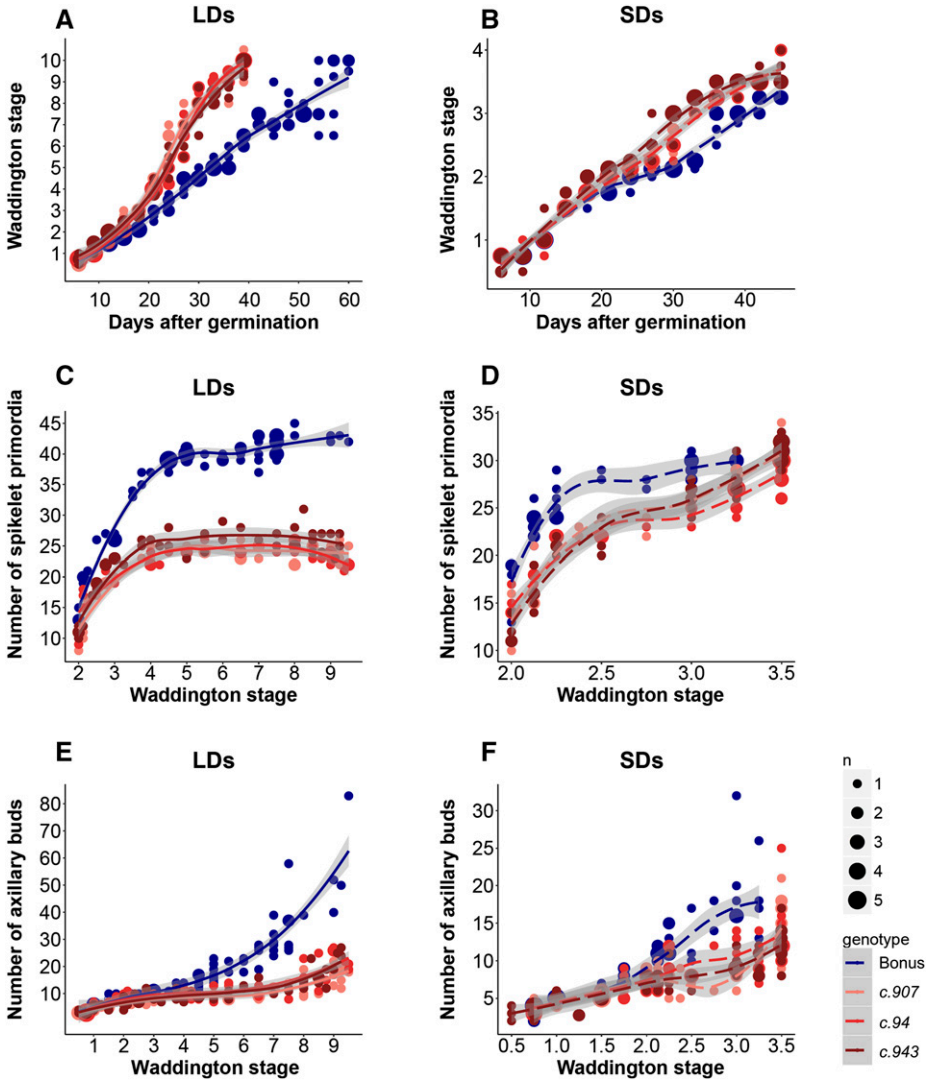

Figure 3. Phenotyping of three *hvcen* mutants (*mat-c.907, mat-c.94, mat-c.943*) and the wild-type Bonus under controlled LD and SD conditions. Development of the MSA and number of spikelet primordia and of axillary buds at different Waddington stages under LDs (A, C, E) and SDs (B, D, F) are shown. The number of spikelet primordia refers to the number of primordia per main spike. The axillary buds scored include all the axillary buds, primary, secondary, and higher order buds. Five or six plants per genotype were dissected at each time point under LDs (16 h light/8 h night) and SDs (8 h/16 h, light/dark). Statistical differences ($P < 0.05$) were calculated using a polynomial regression model at 95% confidence interval (Loess smooth line) shown in gray-shaded regions.

we examined the development of single and double *hvft3 hvcen* mutants under SDs. The *hvft3* single and the *hvft3 hvcen* double mutants did not differ in development and architecture, and both showed a delayed development and an increase in the number of tillers and spikelet primordia (Fig. 4, A–C). Consequently, the *hvcen* allele advanced spikelet initiation and decreased the number of spikelet primordia and axillary buds, but only in the presence of a functional HvFT3. We, therefore, inferred that the photoperiod-independent effects of HvCEN on spikelet initiation are dependent on HvFT3. However, there was no clear effect of HvCEN on the expression of *HvFT3* (Supplemental Fig. S5), suggesting that both interact on the protein level.

Next, we examined if the LD-specific effects on floret development could be explained by the interaction of HvCEN with HvFT1 as *HvFT1* is only expressed under LDs and not SDs. For this purpose, we crossed the *hvcen* mutant with a mutant line carrying a nonfunctional EARLY FLOWERING 3 (HvELF3) allele. Arabidopsis ELF3 is a circadian clock gene that modulates light signal transduction downstream of phytochromes and mediates the circadian gating of light perception and responses (Hicks et al., 1996; Zagotta et al., 1996; Liu et al., 2001). Barley *hvelf3* mutants are characterized by photoperiod-independent expression of *HvFT1* and early flowering (Faure et al., 2012). We confirmed that expression levels of *HvFT1* were comparable between *HvELF3* wild-type plants grown under LDs and *hvelf3* mutant plants grown under SDs (Supplemental Fig. S6). We then examined MSA development in single and double *hvelf3 hvcen* mutants under SDs. The plants carrying *hvelf3* mutations developed significantly faster when compared with those carrying the wild-type *HvELF3* allele irrespective of the *HvCEN* allele (Fig. 4D). More interestingly, variation at HvCEN strongly affected floral development under SDs in the background of the *hvelf3* mutant but had only a minor effect on floral development in *HvELF3* wild-type plants. This suggested that under conditions where *HvFT1* is expressed, either under LDs or in the *hvelf3* mutant background, HvCEN genetically interacted

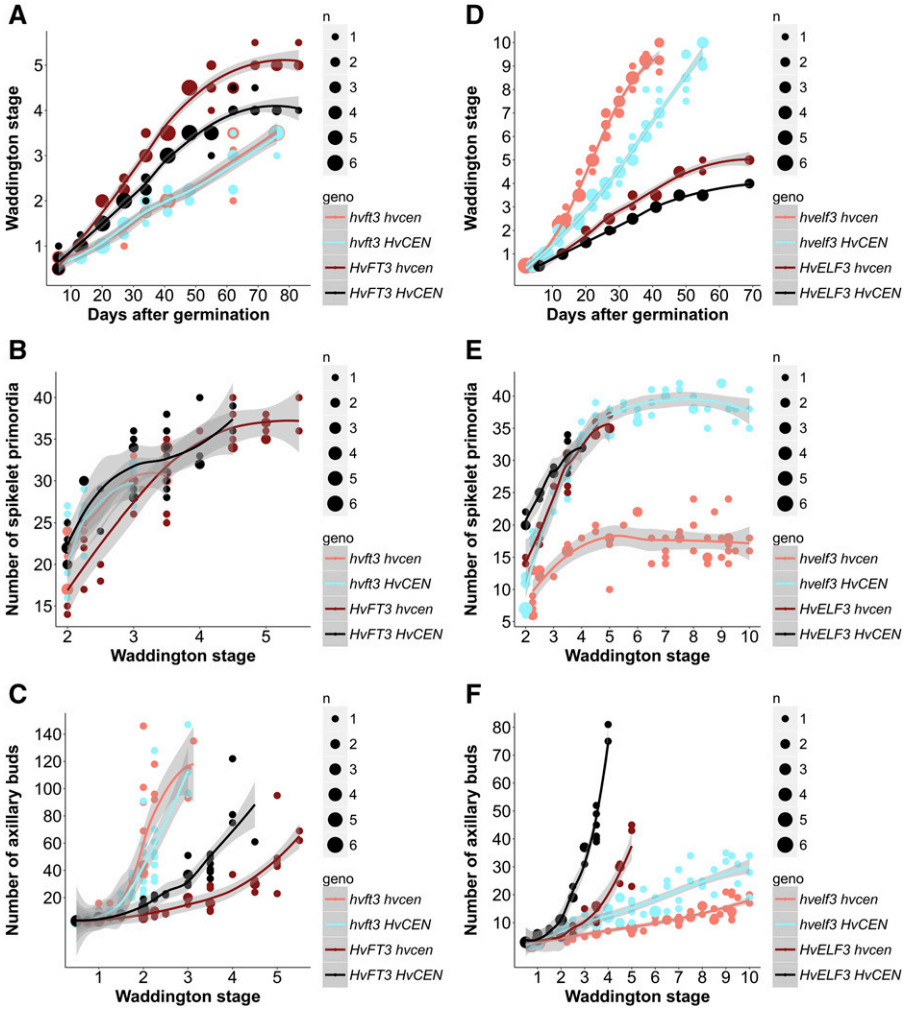

Figure 4. Microscopic phenotypes of *hvft3*, *hvelf3*, and *hvcen* single mutants and *hvft3 hvcen* and *hvelf3 hvcen* double mutants in Bonus under SDs. Development of the MSA, number of spikelet primordia, and number of axillary buds in *HvFT3* or *hvft3* background (A, B, C) and *HvELF3* or *hvelf3* background (C, D, E) at different Waddington stages under SDs (8 h/16 h, light/dark) are shown. The *hvcen* line was *mat-c.907*. The number of spikelet primordia is referring to the number of primordia per main spike. The axillary buds scored include all the axillary buds, primary, secondary, and higher order buds. Three to six plants per genotype were dissected at each time point. Statistical differences ($P < 0.05$) were calculated using a polynomial regression model at 95% confidence interval (Loess smooth line) shown in gray-shaded regions.

with HvFT1 to modulate floral development. The mutation in *hvcen* reduced the number of spikelets per MSA and axillary buds in the background of *hvelf3* as it did in the *HvELF3* background under LDs (Fig. 4, E and F). The genotype and photoperiod-specific expression patterns suggested that the photoperiod-dependent effects of *hvcen* on floret development and spikelet number were likely regulated via *HvFT1*. However, amutations in the clock gene *HvELF3* modify the expression of a large number of genes (Faure et al., 2012), we therefore could not rule out that the *hvelf3*-specific effect of *hvcen* might be caused by genes other than *HvFT1*.

Molecular Characterization of HvCEN

To further characterize the function of HvCEN, we examined the spatial expression patterns of *HvCEN* in the main shoot apex and crown tissue of cv Bonus and cv Bowman by RNA in situ hybridization at the spikelet initiation and stamen primordium stages. *HvCEN* RNA was localized in the AXMs and leaf axils, but no signals were detected in the inflorescence meristems (Fig. 5, A–D; Supplemental Fig. S7). To test if *HvCEN* was also expressed in the inflorescence but at levels too low for detection by in situ hybridization, we dissected the inflorescence meristems only and tested for *HvCEN* expression by real-time quantitative PCR (RT-qPCR). *HvCEN* mRNA was expressed in the inflorescence at both spikelet initiation (W2.0) and stamen primordium stages (W3.5) with a higher level at spikelet initiation (Fig. 5E). These results indicate that HvCEN is expressed in both the AXMs and leaf axils as well as the main inflorescence.

To further understand how HvCEN regulates the development of MSA in a photoperiod-dependent and independent manner, we performed genome-wide transcriptome profiling in developing MSA in two allelic *hvcen* mutants (*mat-c.907* and *mat-c.943*) and the wild type (cv Bonus). We focused on three developmental stages during which genotypes exhibited phenotypic differences under LDs and SDs (Fig. 3; Supplemental Fig. S4), including the vegetative stage (W1.0, MSA enriched tissue), the spikelet initiation stage (W2.0, MSA enriched tissue), and the stamen primordium stage (W3.5, MSA tissue). Transcriptome analysis revealed the expression of 24703 and 25037

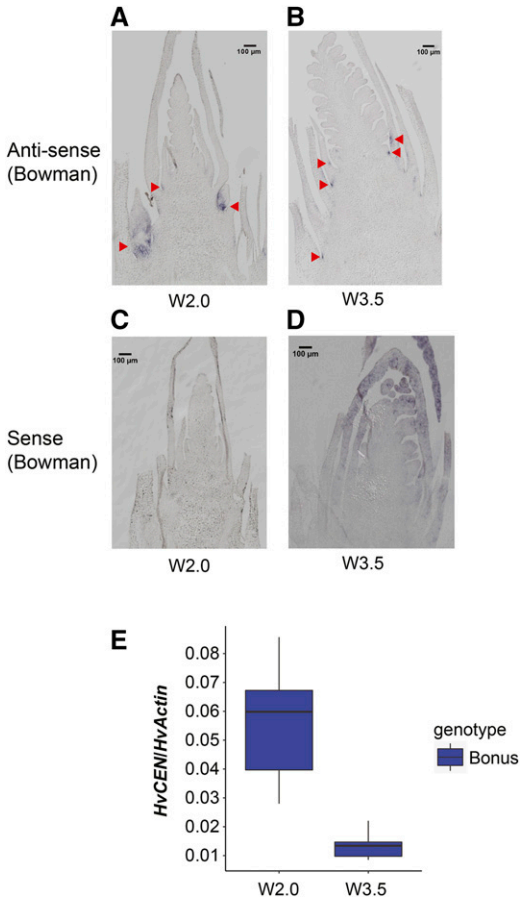

Figure 5. Expression pattern of *HvCEN* under LDs. A and B, RNA in situ hybridization using the antisense probe. Red arrows indicate the *HvCEN* expression domains. C and D, Negative controls using the sense probe of *HvCEN* in the shoot apex of cv Bowman at Waddington stages 2.0 and 3.5. Scale bars = 100 μm. E, Expression of *HvCEN* in the pure inflorescence meristem of cv Bonus. Pure meristems, with six replicates per stage, were obtained by carefully removing leaf primordia and stem tissue beneath the inflorescence under the microscope. LDs are 16 h/8 h light/dark. W, Waddington stage. Error bars = SD.

transcripts, 62.2% and 63.0% of the total number of annotated transcripts in barley (Mascher et al., 2017), at levels greater than 5 counts in at least 2 libraries under LDs and SDs, respectively (Supplemental Table S3). Principle component (PC) analysis on all expressed genes clustered the samples according to the developmental stage under LDs and SDs and separated wild-type and mutant samples at all stages under SDs but not under LDs (Supplemental Fig. S8). To determine differentially expressed transcripts (DETs), we performed individual pairwise comparisons between each mutant (two allelic mutants) with the wild-type background Bonus at each developmental stage (three stages) within each photoperiod treatment (LDs and SDs), yielding 12 sets of DETs. A large number of DETs were identified at the spikelet initiation stage (W2.0) with 3177 DETs in *mat-c.907* and 2876 DETs in *mat-c.943* under LDs and 5200 DETs in *mat-c.907* and 5585 DETs in *mat-c.943* under SDs. At the vegetative stage (W1.0), only 50 DETs in *mat-c.907* and 419 DETs in *mat-c.943* under LDs and under SDs 14 DETs in *mat-c.907* and 17 DETs in *mat-c.943* were found. At the stamen primordium stage (W3.5), we identified 503 DETs in *mat-c.907* and 477 DETs in *mat-c.943* under LDs and 281 DETs in *mat-c.907* and 489 DETs in *mat-c.943* under SDs (Supplemental Fig. S9).

Differences in the number of genes that were affected in the two allelic *hvcen* mutants may be due to other background mutations in the mutants. Variant calling revealed that 12 and 78 transcripts contain mutations in the mutants *mat-c.907* and *mat-c.943*, respectively, compared to Bonus. Among them, only one transcript (*HvCEN*) carried different mutations in both mutants (Supplemental Table S4). In order to minimize possible effects of other background mutations, we focused further analyses on transcripts that were differentially regulated in both *hvcen* mutants, with 33, 1926, and 229 DETs under LDs and 7, 4310, and 117 DETs under SDs at W1.0, W2.0, and W3.5, respectively (Supplemental Fig. S9). Most DETs under both LDs and SDs were observed at W2.0, which corresponded to the developmental stage where the highest expression of *HvCEN* was observed in the MSA (Figs. 5E and 6A; Supplemental Fig. S9). Hierarchical cluster analysis separated the developmental stages on the first PC and the photoperiods on the second PC. Only samples harvested at W2.0 were separated for mutants and wild type (Fig. 6B; Supplemental Fig. S8C). The majority of genes showed photoperiod-specific regulation. At W2.0 ~73% of the DETs were photoperiod specific, whereas at W3.5 92% of the DETs were photoperiod specific (Fig. 6A).

Taken together, HvCEN had the strongest effect on gene expression at spikelet initiation, specifically under SDs. In addition, the majority of transcripts showed a photoperiod- and stage-specific regulation in the mutant and the wild-type plants.

Transcripts Regulated at the Spikelet Initiation Stage in *hvcen* Mutants

Because spikelet initiation was accelerated in the mutants under both photoperiods, we first focused on all transcripts that were regulated at W2.0 independent of the photoperiod. Gene ontology enrichment analysis suggested that HvCEN primarily affected transcripts involved in chromatin modification, ribosome biogenesis, response to cytokinin, cell proliferation, and metabolic and biosynthetic processes (Supplemental Table S5).

Among the genes with roles in chromatin modification (selected genes in Supplemental Table S6), we observed, for instance, the up-regulation of two homologs of Arabidopsis *MULTICOPY SUPRESSOR OF IRA1* (*AtMSI1*), *HORVU5Hr1G084160* (Fig. 7A) and *HORVU5Hr1G093230*. MSI1 is involved in de novo nucleosome assembly during DNA replication and SAM

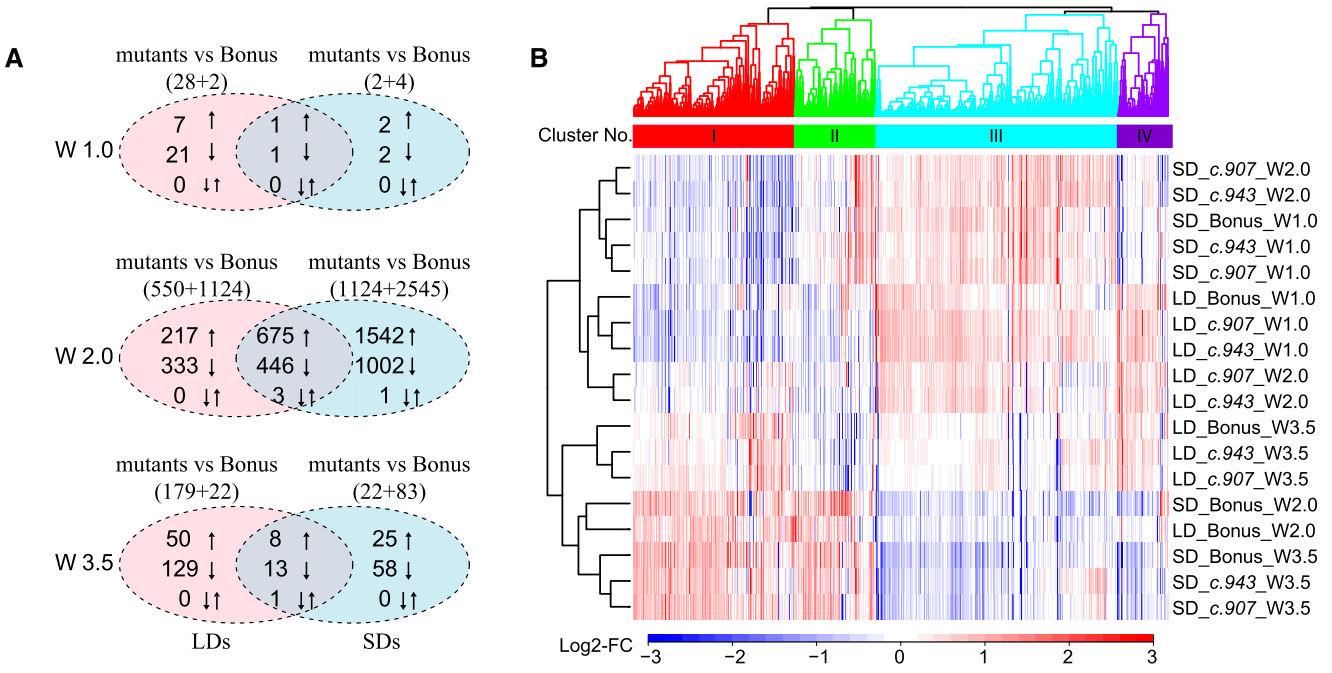

Figure 6. DETs regulated between two *hvcen* mutants (*mat-c.907* and *mat-c.943*) and wild type (Bonus) in at least one photoperiod condition (LD/SD) and coexpression patterns of the DETs. A, Number of DETs regulated in both mutants (*mat-c.907* and *mat-c.943*) compared with wild type (Bonus) under LDs and/or SDs. The red circles display DETs detected under LDs, and blue circles show DETs detected under SDs. B, Heatmap of coexpression clusters for 4527 DETs. Colors represent log2-fold changes (log2-FC) in expression levels relative to the mean transcript abundance across the tested conditions, i.e. apex (enriched) samples of *mat-c.907*, *mat-c.943*, and Bonus grown under LD and SD conditions and harvested at different developmental stages (W1.0, W2.0, W3.5). LDs are 16 h/8 h, light/dark; SDs are 8 h/16 h, light/dark. W, Waddington stage. Transcripts with false discovery rate (FDR) < 0.01 were considered as DETs.

organization and promotes floral transition in Arabidopsis by inducing the expression of *CONSTANS (CO)* and SUPPRESSOR OF OVEREXPRESSION OF CONSTANS (*SOC1*; Bouveret et al., 2006; Steinbach and Hennig, 2014). In addition, the expression of homologs of *PROTEIN ARG METHYLTRANSFERASES* (*AtPRMT5*, *HORVU6Hr1G019540* [Fig. 7A], and *AtPRMT10*, *HORVU7Hr1G020620*) was increased in the mutants compared with wild type. In Arabidopsis, *PRMT* genes promote flowering by mediating the epigenetic silencing of *FLOWERING LOCUS C* (*AtFLC*) and by affecting pre-mRNA splicing (Schmitz et al., 2008; Deng et al., 2010). A putative target of epigenetic factors and repressor of flowering, a homolog of *FLC*, the grass-specific MADS-box gene *HvODDSOC2* (*HORVU3Hr1G095240*), was downregulated in the mutants. In addition, we observed a higher expression of a homolog of *ARABIDOPSIS TRITHORAX-RELATED PROTEIN 6 (ATXR6*; *HORVU6Hr1G011950*; Fig. 7A), which encodes a [Su(var)3-9, Enhancer-of-zeste and Trithorax]-domain protein, a H3K27 monomethyltransferase required for chromatin structure and gene silencing (Jacob et al., 2008). Among the upregulated genes were also ribosomal proteins (selected genes in Supplemental Table S6) with functions in inflorescence development, vascular patterning, and adaxial cell fate, such as two homologs of PIGGYBACK 2 (PGY2, *HORVU0Hr1G006020*; Fig. 7B; *HORVU3Hr1G001140*), and a homolog of PGY3 (*HORVU5Hr1G092630*). A nucleolar GTPase *NUCLEOSTEMIN-LIKE 1 (AtNSN1)*-like transcript (*HORVU2Hr1G016650*; Fig. 7B), which plays a role in the maintenance of inflorescence meristem identity and floral organ development by modulating ribosome biogenesis in Arabidopsis (Wang et al., 2012; Jeon et al., 2015), was upregulated in the mutants. Furthermore, we found DETs with putative roles in cytokinin response and cell cycle regulation (Supplemental Table S6). For example, we observed the up-regulation of a barley 26S proteasome non-ATPase regulatory subunit 8 homolog A (*RPN12a*, *HORVU4Hr1G002140*; Fig. 7C), which regulates cytokinin responses by up-regulating type A Arabidopsis thaliana RESPONSE REGULATOR proteins (*ARRs*), which are in turn negative regulators of cytokinin signaling (Ryu et al., 2009). In addition, barley homologs of type *A* and *B RESPONSE REGULATORS* (*ARR2*, *HORVU5Hr1G097560.5*; *ARR3*, *HORVU2Hr1G077000*, *HORVU3Hr1G108540*; *ARR6*, *HORVU2Hr1G120490*, Fig. 7C) that act as regulators in the two-component cytokinin signaling pathway were up-regulated. In contrast, barley homologs of His kinases and putative cytokinin receptors, *HIS KINASE 3* and *HIS KINASE 4* (*AHK3*, *HORVU3Hr1G094870*, Fig. 7C; *AHK4*, *HORVU6Hr1G077070*), were down-regulated in

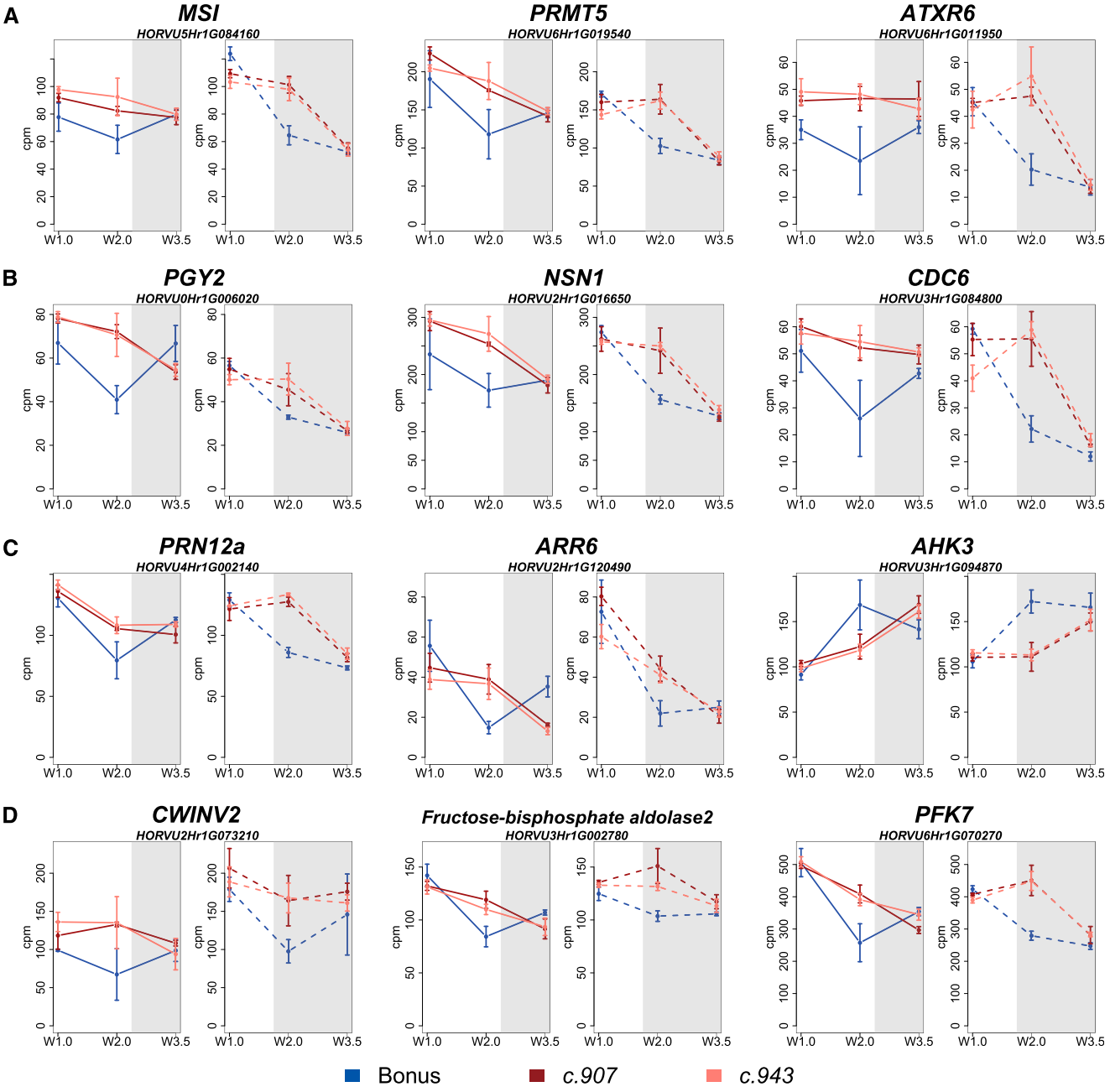

Figure 7. Expression profiles of selected DETs between the *hvcen* mutants (*mat-c.907*, *mat-c.943*) and wild type (Bonus) at W2.0. Genes related to chromatin modification regulation of development, and organ initiation (A); ribosomal proteins, leaf development, leaf patterning (B); regulation of hormone level and hormone response (C); and cellular respiration, sink strength, carbohydrate metabolism, and glycolytic processes (D) under both LDs and SDs. LDs and SDs are shown by white and gray colors. LDs are 16 h/8 h, light/dark; SDs are 8 h/16 h, light/dark; white, light period (16 h); gray, dark period (8 h); W, Waddington stage. Error bars = SD. Transcripts with FDR < 0.01 were considered as DETs. Ten MSAs were pooled for each of the three biological replicates for each time point and genotype.

the mutants compared with wild-type plants. Alterations in the expression of cytokinin response genes were accompanied by the up-regulation in the expression of genes involved in cell division. These included, for example, homologs of *CELL DIVISION CONTROL 6* (*CDC6*, *HORVU3Hr1G084800*, Fig. 7B), *PROLIFERATING CELL NUCLEAR ANTIGEN 2* (*PCNA2*, *HORVU6Hr1G088120*, *HORVU0Hr1G031140*), and *REPLICON PROTEIN A2* (*HORVU6Hr1G094080*). A faster transition to a reproductive MSA and induction of cell cycle genes coincided with the differential expression of genes involved in cellular respiration, including

glycolysis, pyruvate metabolism, and citrate cycle (Supplemental Table S6). For example, transcripts with roles in glycolysis and carbohydrate metabolism were up-regulated in the mutant compared with wild type, i.e. *CELL WALL INVERTASE* 2 (*HORVU2Hr1G073210*; Fig. 7D), a RAFFINOSE SYNTHASE family protein (*HORVU7Hr1G027930*), and a TREHALOSE-6-PHOSPHATASE (*TPS1*, *HORVU1Hr1G013450*). Further proteins with roles in glycolysis, such as a PYRUVATE KINASE family protein (*HORVU3Hr1G039200*), three homologs of FRU-BISPHOSPHATE ALDOLASE 2 (*FBA2*, *HORVU3Hr1G002780*; Fig. 7D; *HORVU3Hr1G088540*, *HORVU3Hr1G088570*), and three homologs of ATP-dependent 6-PHOSPHOFRUCTOKINASES (*PFK2*, *HORVU2Hr1G081670*; *PFK3*, *HORVU3Hr1G070300*; *PFK7*, *HORVU6Hr1G070270*; Fig. 7D) were up-regulated in the mutant versus wild-type plants. The up-regulation of genes involved in cellular respiration might be a consequence of changes in the source sink balance and a stronger energy demand required for the accelerated vegetative to reproductive stage transitions in the mutant plants compared with the wild type. Taken together, HvCEN had the strongest molecular effects on the MSA transcriptome at spikelet initiation, and these involved genes with functions in chromatin remodeling activities, cytokinin and cell cycle, and regulation and cellular respiration independent of the photoperiod.

HvCEN Controls Floral Homeotic Genes under LDs

Spikelet initiation was advanced in the mutants under both LDs and SDs, but only florets developed and set seeds under LDs, whereas the MSAs were aborted under SDs. To gain a better understanding of the photoperiod-dependent effects of HvCEN on floret development, we analyzed the photoperiod-dependent transcripts at the stamen primordium stage (W3.5). The photoperiod-specific DETs, including 179 LD-specific and 83 SD-specific DETs, were enriched for transcripts with functions in reproductive processes, response to stimuli, and cell communication (Supplemental Table S7). Among the 179 LD-specific DETs at W3.5, 50 DETs were up-regulated and 129 DETs down-regulated in the mutants compared with wild type. Among the transcripts (selected genes in Supplemental Table S8) that were up-regulated to a higher extent in the mutants compared with wild type only under LD were *HvCEN* (*HORVU2Hr1G072750*; Fig. 8A) and flowering promoting genes such as barley homologs of *SOC1* (*HORVU1Hr1G051660*; Fig. 8A), *AGAMOUS-LIKE6* (*AGL6*, *HORVU6Hr1G066140*), and *FLOWERING PROMOTING FACTOR 1* (*HORVU2Hr1G007350*; Fig. 8A). In addition, we observed the LD-dependent up-regulation of transcription factors that act in a combinatorial manner to achieve floral patterning in Arabidopsis (Coen and Meyerowitz, 1991). These are designated as class A, B, C, and E genes and, except for the class A gene *AP2*, encode members of the MADS intervening keratin-like and C-terminal type of MADS-box transcription factors. A class A protein, *AP1*-like (*HvBM8, HORVU2Hr1G063800,* FDR < 0.05; Fig. 8C; Supplemental Table S9), and a class B like gene, *PISTILLATA (PI)-like (HORVU1Hr1G063620,* FDR < 0.05; Fig. 8C; Supplemental Table S9*),* were up-regulated in the mutant lines under LDs but not SDs. In addition, the mutations in HvCEN caused an up-regulation of five E class genes, the *SEP*-like genes (*SEP1*, *HORVU7Hr1G025700*, *HORVU5Hr1G095710*; *SEP2, HORVU4Hr1G067680*; *SEP3, HORVU7Hr1G054220, HORVU5Hr1G076400,* FDR < 0.05) at the stamen primordium stage (Supplemental Table S9; Fig. 8B). An ABERRANT PANICLE ORGANIZATION (*APO1*)-like transcript (*HORVU7Hr1G108970*) was down-regulated in the mutants compared with wild type. Interestingly, the ABERRANT PANICLE ORGANIZATION protein positively controls spikelet number by suppressing the precocious conversion of inflorescence meristems to spikelet meristems in rice (Ikeda et al., 2007). In addition, barley homologs of a *SWEET* Suc transporter (*HORVU5Hr1G076770*; Fig. 8C), of a GLYCOGEN SYNTHASE (*HORVU2Hr1G106410*), and a TREHALOSE-6-PHOSPHATE PHOSPHATASE (*HORVU6Hr1G074960*) were up-regulated specifically at W3.5 in the mutants compared with the wild type. Likewise, a barley homolog of a SHAGGY-related kinase (*HORVU3Hr1G034440*) required for the establishment of tissue patterning and cell fate determination and a KNOTTED1-like homeobox gene (*HORVU7Hr1G114650*) involved in meristem differentiation were up-regulated in the mutants at W3.5 under LDs.

Under SD, 83 DETs were detected at W3.5, and 58 among them were down-regulated and 25 up-regulated in the mutants compared with wild type. Among the upregulated genes (selected genes in Supplemental Table S8), we identified a number of stress-related genes involved in detoxification such as a stress responsive A/B Barrel Domain protein (*DABB*, *HORVU0Hr1G011450*; Fig. 8D) and a homolog of *ACYL-COA-BINDING PROTEIN 6* (*AtACBP6*, *HORVU7Hr1G008320*; Fig. 8D). Furthermore, we recorded the mutant-specific up-regulation of transcripts with roles in cellular transport, such as a homolog of *CYCLIC NUCLEOTIDE-GATED ION CHANNEL2 (AtCNGC2, HORVU5Hr1G096440*; Fig. 8D*)*, building nonselective cation channels and of *PLASMA MEMBERANE INTRINSIC PROTEIN 3 (AtPIP3, HORVU5Hr1G125600)* forming water channels (Fig. 8C). Finally, proteins with roles in starch and sugar metabolism, such as a TREHALOSE-6-PHOSPHATE PHOSPHATASE (TPPH, *HORVU5Hr1G058300*), a SUC SYNTHASE (*HORVU7Hr1G033230*), and a UDP-GLC 4-EPIMERASE (*HORVU7Hr1G053260*), showed a stronger up-regulation in the wild type than the mutants.

Taken together, the LD-specific expression patterns of floral homeotic genes with putative functions in inflorescence, spikelet, and flower development were linked to the differential floret development of mutants and wild type under LDs. Under SDs, the *hvcen* mutant lines were characterized by the differential regulation of

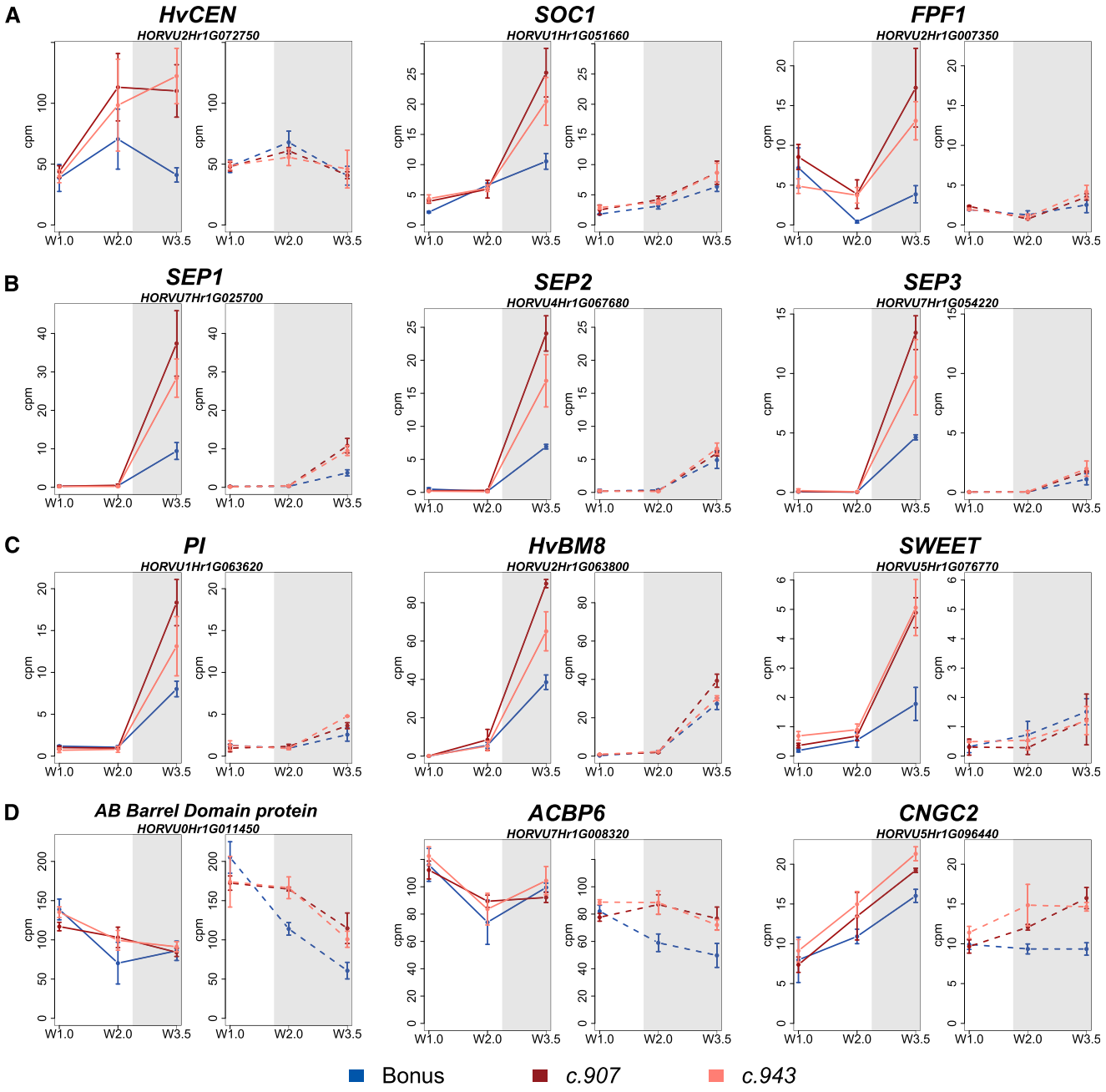

Figure 8. Expression profiles of selected DETs between the *hvcen* mutants (*mat-c.907*, *mat-c.943*) and wild type (Bonus) at W3.5 under both LDs and SDs. A, Transcripts (selected genes in Supplemental Table S8) up-regulated to a higher extent in the mutants compared with wild type only under LD. B and C, Floral homeotic genes and SWEET Suc transporter upregulated in the mutants compared with wild type under LDs and SDs. D, transcripts down-regulated over development under SDs and higher expressed in the mutants vs wild type. LDs and SDs are shown by white and gray colors. LDs are 16 h/8 h, light/dark; SDs are 8 h/16 h, light/dark; white, light period (16 h); gray, dark period (8 h); W, Waddington stage. Error bars = SD. Ten MSAs were pooled for each of the three biological replicates for each time point and genotype. *FPF1*, *FLOWERING PROMOTING FACTOR 1*; *AB*, *ALPHA/BETA BARREL* domain protein; *ACB*, *ACYL-COA-BINDING PROTEIN 6* (*AtACBP6*); *CNG*, *CYCLIC NUCLEOTIDE-GATED ION CHANNEL2* (*CNGC2*).

genes implicated in abiotic stress responses, in cellular transport, and carbohydrate metabolism.

DISCUSSION

In the present work, we analyzed induced *hvcen* mutants to dissect the effects of HvCEN on spike development and plant architecture under different photoperiods and to identify potential molecular targets of HvCEN in the MSA. Mutations in HvCEN accelerated spikelet initiation under LDs and SDs, whereas subsequent floral development required LDs. Therefore, HvCEN showed stage and photoperiod-dependent effects on the development of the MSA. Previous studies have already indicated that spikelet initiation occurs under LDs and SDs, whereas floral development requires LDs in spring barley genotypes (Digel et al., 2015). Floral development, but not spikelet initiation, requires the expression of *HvFT1* and *TaFT* in barley and wheat, respectively (Pearce et al., 2013; Digel et al., 2015). Spikelet initiation occurs in the absence of *FT1* expression, likely promoted by *FT3*. However, the timing of spikelet initiation is affected by variation in *FT1* expression (Digel et al., 2015; Dixon et al., 2018).

In Arabidopsis, TFL1 acts antagonistically to the FT protein to repress floral transition and development (Ruiz-García et al., 1997; Jaeger et al., 2013). In addition, rice TFL1-like proteins, such as RICE CENTRORADIALIS (RCN), compete with the rice FT ortholog Hd3a for the binding activities of the 14-3-3 protein, thereby antagonizing the activities of the florigen (Kaneko-Suzuki et al., 2018). Therefore, we also tested if HvCEN genetically interacts with HvFT1 and HvFT3, which affect different stages of preanthesis development (Yan et al., 2006; Casao et al., 2011; Halliwell et al., 2016; Mulki et al., 2018). Although HvFT1 primarily accelerates floral development under LDs (Hemming et al., 2008; Sasani et al., 2009), HvFT3 controls spikelet initiation under LDs and SDs (Mulki et al., 2018). The double mutant *hvcen hvft3* did not differ in the timing of spikelet initiation under SDs from the *HvCEN hvft3* line, suggesting that the repressive effect of HvCEN on the timing of spikelet initiation depends on a functional *HvFT3* gene. In contrast to *HvFT3*, *HvFT1* is only expressed under LDs, and *HvFT1* expression is crucial for floral development and flowering (Digel et al., 2015). Consequently, we tested if the LD-specific effect of HvCEN on floral development was dependent on *HvFT1* expression. For this purpose, we analyzed an *HvCEN hvelf3* single and *hvcen hvelf3* double mutant that both expressed *HvFT1* under SDs to similar levels as seen under LDs. The strong delay in inflorescence development and higher number of the spikelets in the *hvelf3* single mutant as compared with the *hvcen hvelf3* double mutant under SDs indicated that the repressive effect of HvCEN on floral development depended on *HvFT1* expression in the *hvelf3* mutant. In addition, the interaction between HvCEN and FT1 had a strong effect on the determination of spikelet primordia number. However, as many light-dependent transcripts are misregulated in the *hvelf3* mutant (Faure et al., 2012), we cannot rule out that other genes influenced the observed phenotype. Our results suggested that HvCEN genetically interacted with different *FT*-like genes in the shoot apical meristem to control different phases of inflorescence development: with HvFT3 to control spikelet initiation, and with HvFT1 to control floral development. The photoperiod-specific effects of HvCEN are therefore likely caused by the photoperiod-specific expression of its putative competitors HvFT3 and HvFT1.

The *hvcen* mutants were altered in different shoot architecture traits, including the number of leaves on the main culm, leaf length, the number of tillers per plant, and the number of seeds per spike. The mutant plants developed 1 to 2 fewer leaves on the main culm under LDs and SDs, possibly as a consequence of the earlier transition from a vegetative to a reproductive meristem. Because AXMs initiate in the leaf axils, a reduction in the number of leaves may have caused the reduction in tiller number observed in the mutant lines. In addition, the leaves in the *hvcen* mutants were shorter, indicating that leaf size is controlled by HvCEN-dependent progression of plant development. It has already been demonstrated that flowering time genes may affect leaf size in barley by affecting the duration of leaf growth and consequent variation in leaf cell number (Digel et al., 2016). The earlier termination of leaf growth in the *hvcen* mutants was matched by an earlier termination of spikelet induction. However, the barley *hvcen* mutants did not form a terminal spikelet as has been described for the Arabidopsis *tfl1* mutant (Shannon and Meeks-Wagner, 1991). Nevertheless, the mutation in *hvcen* reduced the period of spikelet primordia initiation and thereby decreased the number of spikelets on the MSA. The wild type reached the maximal number of spikelets at awn primordium stage as observed in previous studies (Riggs and Kirby, 1978; Waddington et al., 1983; Kirby and Appleyard, 1987; Kernich et al., 1997; Alqudah and Schnurbusch, 2014), whereas the *hvcen* (*mat-c*) mutants stopped to produce further spikelets at the pistil primordium stage under inductive LD conditions. It has already been shown before that variation in the developmental timing of the early reproductive phase has strong effects on the number of spikelet primordia on the MSA (Campoli and von Korff, 2014; Digel et al., 2015; Ejaz and von Korff, 2017). For instance, in the presence of a wild-type *PPD-H1* allele, the development of the MSA is accelerated, and this is associated with a reduction in number of spikelet primordia and final grain number per main spike (Digel et al., 2015). In wheat, Alvarez et al. (2016) observed an acceleration of flowering time and an associated reduction in spikelet number in an *elf3* mutant. Both PPD-H1 and HvELF3 likely affect developmental timing and spikelet number by inducing or repressing *HvFT1*, respectively. Taken together, the pleiotropic phenotypes of the *hvcen* mutants suggested that changes in the HvFT1/HvCEN ratios may

control meristematic activity or its termination in different meristems of the barley shoot as has been proposed for tomato (*Solanum lycopersicum*; Krieger et al., 2010; Jiang et al., 2013; Lifschitz et al., 2014; Park et al., 2014). However, the molecular basis for these coordinated effects on meristems remain poorly understood.

In Arabidopsis, *TFL1* mRNA is expressed in young AXMs but later becomes restricted to the central inflorescence meristem (Shannon and Meeks-Wagner, 1991; Bradley et al., 1997; Wigge et al., 2005; Conti and Bradley, 2007). By contrast, *HvCEN* mRNA signals were detected primarily in the AXMs, and expression levels were low in the shoot apex despite the strong effect of mutations in HvCEN on developmental timing and spike morphology, i.e. the number of spikelets and seeds per spike. Similarly, expression of the HvCEN homologs RCN1-4 in rice was not detected in the SAM, but in the vasculature of the subtending stem and young primordia and leaf blade (Kaneko-Suzuki et al., 2018). However, the authors demonstrated that the RCN protein is transported through the phloem to the inflorescence meristem where it controls phase transition and inflorescence determinacy. Consequently, HvCEN protein might also travel to the inflorescence meristem where it acts on spike development. Accordingly, the largest number of differentially transcribed genes was detected at the spikelet initiation stage when the SAM switches from vegetative to reproductive growth. This acceleration of spikelet initiation in the *hvcen* mutants under LDs and SDs coincided with the differential regulation of transcripts associated with chromatin modifications. Epigenetic genes putatively upstream of floral regulators included, for example, MSI1, which is part of the evolutionarily conserved Polycomb group chromatin-remodeling complex and controls spatial and temporal expression of several homeotic genes that regulate plant development and organ identity (Chanvivattana et al., 2004; Hennig et al., 2005; Derkacheva et al., 2013; Steinbach and Hennig, 2014). Similarly *PRMT*-like genes were upregulated in the mutants, and these control the epigenetic silencing of the floral repressor *FLC* and flowering time in Arabidopsis (Niu et al., 2007; Pei et al., 2007; Wang et al., 2007; Schmitz et al., 2008). The up-regulation of *PRMT*-like genes was linked to a down-regulation of a putative repressor of flowering and homolog of *FLC*, *HvODDSOC2*, suggesting that its expression might also be controlled epigenetically. Further, we recorded a strong up-regulation of Trithorax-like proteins that act as H3K27 methyltransferases required for transcriptional repression in Arabidopsis (Jacob et al., 2009). HvCEN-dependent regulation of epigenetic regulators in the MSA of barley, specifically at spikelet initiation, suggested that the transition from vegetative to reproductive meristem requires strong reprogramming of transcriptional networks by epigenetic modifiers. These modifiers and their role for developmental transitions in barley await further functional characterization.

Further, we observed the up-regulation of genes involved in cell cycle regulation, cytokinin signaling, and response and many ribosomal proteins that are thought to control cellular growth (Naora, 1999; Bhavsar et al., 2010; Schaller et al., 2014). The up-regulation of ribosomal proteins in the mutants was specific for the spikelet initiation stage, suggesting that the transition from a vegetative to a reproductive meristem requires a strong increase in translational efficiency and de novo protein synthesis. However, several of the ribosomal proteins up-regulated in the mutants may have more specific effects on organ development as these are also described as important regulators of leaf and inflorescence development, vascular patterning, and phase change, such as *RPS13*-like and *PGY*-like genes (Ito et al., 2000; Pinon et al., 2008). Spikelet initiation also coincided with the up-regulation of genes involved in carbon metabolism, glycolysis, cellular respiration, and tricarboxylic acid cycle. These transcripts may be important to prepare the plant for the subsequent fast inflorescence growth and increased energy demand. Ghiglione et al. (2008) have demonstrated that fast growing wheat inflorescences show strongly reduced soluble carbohydrate levels as compared with slowly developing spikes and suggested that these fast-growing tissues suffer from carbohydrate starvation. Consequently, the up-regulation of cellular respiration genes was possibly important to allow for a higher energy supply to the developing organs in the fast-growing mutants.

In contrast with spikelet initiation, floral development was photoperiod dependent, and the majority of transcripts in the MSA were regulated by HvCEN only under LDs. In particular, floral homeotic genes were primarily regulated under LD conditions by HvCEN, and these included homologs of floral patterning transcription factors designated as class A, B, and C genes (for review, see Theissen, 2001). The mutations in HvCEN caused an up-regulation of five E class, *SEP*-like, genes; a class B gene (*PI*, *OsMADS4*); and one *AP1*-like gene (*HvBM8*) at the stamen primordium stage. In rice, the *SEP*-like gene *OsMADS34* (*PANICLE PHYTOMER2*) is important for controlling inflorescence and spikelet development (Gao et al., 2010; Kobayashi et al., 2010), whereas the other *SEP*-like genes *OsMADS1*, *OsMADS5*, *OsMADS7*, *OsMADS8*, and *OsMADS34* control the development of different floral organs (Malcomber and Kellogg, 2005; Zahn et al., 2005; Arora et al., 2007). Interestingly, the barley homolog of *OSMADS34* was regulated by HvCEN under both photoperiods, whereas the other *SEP*-like genes were controlled by HvCEN only under LDs. This suggested that genes important for floral development but not those involved in spikelet initiation were LD dependent. The repression of these genes by HvCEN is not only essential to delay floral development but also to prolong leaf initiation and leaf maturation, probably as a strategy to match vegetative and reproductive development of the plant.

MATERIAL AND METHODS

Germplasms of *hvcen* (*praematurum-c, mat-c*), *hvelf3 hvcen*, and *hvft3 hvcen* Double Mutants

All barley (*Hordeum vulgare*) mutants and parental lines were obtained from the Nordic Gene Bank (NordGen; http://www.nordgen.org/). The 21 allelic *hvcen* mutants were originally generated using different mutagens in various barley spring cultivars (wild-type parents): Bonus, Foma, Frida, Kristina, and Semira (Franckowiak and Lundqvist, 2011; Comadran et al., 2012; Matyszczak, 2014; Supplemental Table S1; Supplemental Fig. S2). The different mutants were characterized by distinct changes in the gene body, including premature stop codons, changes in splice sites, amino acid replacement, frameshift, and whole gene deletions (Comadran et al., 2012). The mutation in *mat-c.770* introduced a stop codon, resulting in a truncated protein. Mutations in *mat-c.94*, *mat-c.1111*, and *mat-c.1114* caused splice site changes. Amino acid substitution at conserved sites were detected in *mat-c.32*, *mat-c.770*, *mat-c.907*, *mat-c.943*, *mat-c.913*, *mat-c.93*, *mat-c.400*, *and mat-c.1115* (Supplemental Table S2). The *mat-c.1109* genotype carried a 1-bp deletion that resulted in a frame shift. Sanger Sequencing of HvCEN in *mat-c.1118* revealed a 12-bp deletion (GATGCAAA-CAAT) including 2 bp from the end of the 4th exon and 10 bp from the untranslated region (10 bp), leading to a larger protein consisting of 229 instead of 173 amino acids (Supplemental Fig. S2). The *mat-c.16*, *mat-c.19*, *mat-c.1096*, *mat-c.1107*, *mat-c.1102*, *mat-c.1108*, and *mat-c.1120* mutants were putative deletion mutants as *HvCEN* could not be amplified in these genotypes. In addition, two backcross-derived introgression lines *BW508*, with an introgression of *mat-c.19*, and *BW507* with an introgression of *mat-b.7* in the background of Bowman, were analyzed (Druka et al., 2011). *BW507* likely contains a large deletion of *HvCEN* since no amplicons of this gene were found (Matyszczak, 2014). The effects of a single amino acid substitution in the point mutants were evaluated by PROVEAN (Protein Variation Effect Analyzer; http://provean.jcvi.org), which computationally predicts the influence of alternations in amino acids on the biological function of the protein (Supplemental Table S2). The program assesses the functional effects of protein variation using an alignment-based score (PROVEN score) that measures the change in sequence similarity between a query sequence and its variants to a homologous protein sequence (Choi et al., 2012).

To determine if HvCEN interacts with HvFT1 and HvFT3 genetically, *hvelf3 hvcen* (with *HvFT1* expression under SDs) and *hvft3 hvcen* double mutants were produced. The *hvelf3 hvcen* double mutants were derived from the cross of the *hvcen* mutant in Bonus (*mat-c.907*) with the *hvelf3* mutant in Bonus (*mat-a.8*, NGB110008). Three F2 progenies verified as homozygous *hvelf3 hvcen* double and two as *hvelf3 HvCEN* single mutants were propagated. F4 plants from these selected five lines were grown and dissected in a controlled climate chamber under SD conditions (8 h/16 h, light/dark, 20°C/18°C).

To obtain *hvft3 hvcen* double mutants, the *hvcen* mutant (*mat-c.907*) in the Bonus background was crossed to an introgressed line carrying a natural mutation in *hvft3* in the background of Golden Promise. This introgression line was an F3 progeny derived from crosses between the winter barley cultivar Igri and the spring cultivar Golden Promise. Specifically, the introgression line carried a nonfunctional *hvft3* allele from Igri and the natural mutation at *Ppd-H1*, a deletion in the first regulatory intron of *VRN1*, and a deletion of the *VRN2* locus from Golden Promise. This introgression line shows a reduced photoperiod response and does not require vernalization. By genotyping, three *F2* lines carrying homozygous *hvft3 hvcen* double mutations and two *hvft3 HvCEN* progenies were identified and propagated.

Plant Growth Conditions and Phenotyping in Outdoor Conditions and Climate Chambers

All mutants and their parental lines (Supplemental Table S1) were evaluated under outdoor conditions over 2 consecutive years for the number of tillers and spikelets per main spike, plant height, and flowering time. Plants were sown in 96-well trays in mid-February in 2014 and early March in 2015, germinated in the greenhouse and then transferred outside (Cologne, Germany). After 5 weeks in 2014 and 3 weeks in 2015, plants were transferred to 12 L pots with one plant per pot during late March, each filled with a custom-made peat and clay soil mixture (EinheitsErde ED73 Osmocote, Einheitserdewerke Werkverband e.V., Sinntal-Altengronau, Germany) containing a long-term fertilizer. The pots were arranged in 22 rows with a distance of 1 m between rows where each row contained 54 pots with a distance of 10 cm. To avoid edge effects, the plot was surrounded by border pots containing cv Morex barley plants. The plot was irrigated by a sprinkling robot and treated with additional fertilizer or pesticides when necessary. Flowering time was scored as the time from sowing to heading, when the awns emerge from the flag leaf of the main culm. Tiller number was recorded at heading, whereas the number of grains per main spike and plant height (soil to base of topmost spike) were measured at full maturity, 2 weeks before harvest. The numbers of *mat-c* mutants and wild-type plants grown in each year are indicated in Supplemental Table S1.

In parallel, phenotyping was conducted in environment-controlled growth chambers using selected *hvcen* mutants. Specifically, three *hvcen* mutants in the Bonus background (*mat-c.907*, *mat-c.94*, and *mat-c.943*) and Bonus were grown in 96-well trays using "Mini Tray" (Einheitserde) soil. To synchronize germination, the trays were stratified in dark at 4°C for 3 d followed by growth under LDs (16 h, 22°C day; 8 h, 18°C night) or SDs (8 h, 22°C day; 16 h, 18°C night). The developmental stage of the MSA was determined using the Waddington quantitative scale of shoot apex development that is based on the progression of spike initiation and then the most advanced floret primordium and pistil of the inflorescence (Waddington et al., 1983). Five to six individual plants for each focal accession were scored for their MSA development every 3 d, and the number of spikelet primordia per main spike, the number of axillary buds, and leaf primordia number were scored during the dissection. The axillary buds scored include all the axillary buds, primary, secondary, and higher order buds. Each leaf was dissected to see the axillary bud under the leaf sheath. Leaf size and visible leaf number on the main culm were scored in 20-well trays as described by Digel et al. (2016).

The *hvelf3 hvcen* and *hvft3 hvcen* double mutants and their control or parental lines were scored for differences in preanthesis development, number of spikelet primordia per main spike, and number of axillary buds, including all the axillary buds, primary, secondary, and higher order buds by dissecting the lines every 2/4 d (*hvelf3 hvcen)* or weekly (*hvft3 hvcen)* in 96-well trays under SDs.

Statistical Analysis

One-way ANOVA was conducted followed by a post hoc Tukey honestly significant difference test to test for differences in flowering time, plant height, tiller number, and number of seeds per main spike of the mutants compared with their respective parental lines. In addition, a one-way ANOVA was conducted to compare *HvFT3* expression in *HvCEN* wild-type and *hvcen* mutant backgrounds. In the dissection experiments, differences between the parental lines, the mutant, and double mutant lines were revealed by calculating a polynomial regression model at a 95% confidence interval (Loess smooth line).

RNA Isolation and Sample Preparation for RNA Sequencing

Total mRNA was isolated from plants grown under LDs and SDs. MSA-enriched tissues were harvested and pooled for three distinct developmental stages: the vegetative stage (W1.0), the spikelet initiation stage (W2.0), and the anther primordium stage (W3.5; Waddington et al., 1983). The samples were harvested 2 h before dark under both LD and SD conditions. To enrich shoot apex-specific mRNA, leaves surrounding the MSA were removed manually using a microsurgical stab knife (5-mm blade at 15° [SSC#72-1551]). The enriched MSA tissue was cut from the base of the MSA and still included leaf primordia. At least 10 MSAs were pooled for each of the three biological replicates per time point. All samples harvested for RNA extraction were frozen immediately in liquid nitrogen and stored at −80°C. Total mRNA was extracted using TRIzol reagent (Invitrogen) and further purified using an RNA easy Micro Kit (Qiagen). The residual DNA was removed using a DNA-free kit (Ambion), and the quality of the RNA was assessed using a bioanalyzer (Agilent 2100 Bioanalyzer). The Illumina complementary DNA (cDNA) libraries were prepared according to the TruSeq RNA sample preparation (version 2; Illumina). A cBot (Illumina) was used for clonal sequence amplification and generation of sequence clusters. Single-end sequencing was performed using a HiSeq 3000 (Illumina) platform by multiplexing 8 libraries resulting in ~ 18 million reads per library. The requested single end read length was 100 bp for LD samples and 150 bp for SD samples. The initial quality control of the raw reads was performed using the FastQC software (version 0.10.1; http://www.bioinformatics.bbsrc.ac.uk/projects/fastqc/).

Transcriptome Profiling and Variant Calling

The obtained RNA sequencing reads were mapped to a barley High Confidence (HC) transcripts reference (Mascher et al., 2017) using Salmon in quasi-mapping-based mode. When the quasi-mapping-based index was being built, an auxiliary k-mer hash over k-mers of length 31 was used. U (unstranded single end read) was chosen as library type to quantify the reads of each library. The expected number of reads (NumReads) that have originated from each transcript given the structure of the uniquely mapped and multimapped reads and the relative abundance estimates for each transcript and transcripts per million values were extracted using Salmon (Patro et al., 2017). Transcripts with expression levels greater than 5 NumReads in at least two libraries under LDs or SDs were retained. Tables with expected NumReads (raw counts) and expression levels (normalized cpm) are provided in a supplementary table (Supplemental Table S10).

To identify DETs, pairwise comparisons, including *mat-c.907* vs Bonus and *mat-c.943* vs Bonus at each stage and photoperiod condition were done using the R bioconductor package Limma-vroom with a Benjamin & Hochberg adjustment for multiple testing (FDR; Ritchie et al., 2015). The comparisons between the stages and between the photoperiods were not conducted to avoid false positive DETs due to differences in the sample types and potential effects of diurnal gene expression differences between photoperiods. The FDR value of 0.01 was used as initial cutoff value for the selection of DETs. In the end, the DETs were extracted per mutant per developmental stage per photoperiod. To minimize the background mutation effects in the two *hvcen* mutants, the DETs regulated in both mutants were focused on compared with wild type. To visualize the number of genotype- or stage- or photoperiod-dependent DETs, Venn diagrams were drawn using the R package VennDiagram (Chen and Boutros, 2011). The DETs that were observed in both mutants were considered as candidate DETs regulated by HvCEN under each condition. Total, 4527 DETs regulated in the two *hvcen* mutant at least at one stage compared with wild type under LDs or SDs were obtained. The expression patterns were then examined using hierarchical cluster analysis (using Pearson correlation coefficients) and principle component analysis of the DETs with R.

To determine which gene categories were enriched under each treatment, de novo Gene Ontology (GO) annotations were first produced for High Confidence (HC) transcripts using Blast2Go local blast (e value cutoff 1×10^{-5}; Conesa et al., 2005). To assess the effect of HvCEN on biological process, the overrepresentation analysis of particular GO terms was performed based on the Fisher's Exact Test (significant cutoff 0.05) using TopGo package in R (Alexa et al., 2006). The redundant GO categories were removed by first filtering annotated transcripts and allowing similarity as 0.5 (Supek et al., 2011). Then the representative GO categories were retained by keeping the enriched transcripts number ≥ 10 and ≥ 5 at W2.0 and W3.5, respectively.

Variant calling to verify the HvCEN mutation in *mat-c.907* and *mat-c.943* and evaluate the number of mutated transcripts in the RNA sequencing reads was done as described in van Esse et al. (2017). Briefly, RNA sequencing reads were mapped to a barley High Confidence (HC) coding sequence reference (Mascher et al., 2017) using Burrows-Wheeler-Aligner using maximal exact matches (version 0.7.15; Li, 2013), allowing a mismatch penalty of 3. Mapping was evaluated using PicardTools (version 1.1.00; http://picard.sourceforge.net) CollectAlignmentSummaryMetrics, and SAMtools (version 1.1.3; Li et al., 2009) was used to determine the number of reads mapped with good mapping quality scores (MAPQ > 1). Read duplicate removal and indel realignment were done using PicardTools MarkDuplicates and GATK IndelRealigner (version 3.1-1; McKenna et al., 2010), respectively. Variant calling was done with GATK UnifiedGenotyper using 30.0 as a minimum confidence threshold and 10.0 for emitting of called single nucleotide polymorphisms and 1 for ploidy. Filtered variants with a depth of coverage ≥ 100, a quality of the assigned genotype ≥ 98, and a value of Phred-scaled likelihood ≥ 2000 were taken into consideration. Mutation types included single nucleotide polymorphism and insertion/deletion. The number of mutations and number of mutated transcripts were summarized in Supplemental Table S3.

Gene Expression using RT-qPCR and RNA in Situ Hybridization

RNA was isolated from leaf tissues harvested from plants grown under LD and SD conditions. Under LD conditions, the second youngest leaf on the main shoot of Bonus (*HvCEN HvELF3*) and *mat-c.907* (*hvcen HvELF3*) at W3.5 was harvested at 2 h before dark. Under SD conditions, the second youngest leaf of three *hvcen hvelf3*, two *HvCEN hvelf3*, *mat-a.8* (*HvCEN hvelf3* -3), *mat-c.907*, and Bonus were harvested 7 h after the beginning of the dark period at the four- to five-leaf stage. Total RNA extraction, first-strand cDNA synthesis, and RT-qPCR were performed as described in Campoli et al. (2012). The primer for *HvFT1* expression is listed in Supplemental Table S10. Two technical replicates were used for each cDNA sample, and starting amounts for each data point were calculated based on the titration curve for each target gene and the reference (*HvACTIN*) gene using the LightCycler 480 Software (Roche; version 1.5).

The expression of *HvCEN* (*HORVU2Hr1G072750.4*) was detected using RNA in situ hybridization on SAMs of Waddington stages W2 and W3.5 as described in Kirschner et al. (2018). The probes were prepared using the whole gene sequences followed by carbonate hydrolysis to ~200 bp fragments. The antisense probe was used for detecting *HvCEN* expression, and the sense probe was used for the negative control.

Images were taken using a plan-neofluar 10× objective with a numerical aperture of 0.30 using the Zeiss Axioskop light microscope, and image processing, i.e. stitching, was performed with the Stitching Plugin in Fiji (Preibisch et al., 2009; Schindelin et al., 2012).

Data availability was Illumina data in the European Short Read Archive: E-MTAB-7807.

Accession Numbers

Accession Numbers of major flowering time genes are listed in Supplemental Table S10.

Supplemental Data

Supplemental Figure S1. Seed parameters of *hvcen* (*mat-c*) mutants trialled under outdoor condition.

Supplemental Figure S2. The mutation sites of the 14 *mat-c* mutants on the schematic structure of the *HvCEN* gene.

Supplemental Figure S3. Determinate spike with a terminal spikelet in wheat (Chinese Spring) and indeterminate spike without terminal spikelet in barley (*mat-c.907* and Bonus). W: Waddington stage; white bar: 1 mm.

Supplemental Figure S4. Leaf length and number of leaves on the main culm of *hvcen* mutants (*mat-c.907, mat-c.94, mat-c.943*) and Bonus under LDs and SDs.

Supplemental Figure S5. *HvFT3* expression in leaves of Bonus, *mat-c.907* and *mat-c.943* at W2.0 and W3.5 under SDs.

Supplemental Figure S6. *HvFT1* expression in leaves.

Supplemental Figure S7. Expression pattern of *HvCEN* in cv Bonus under LDs.

Supplemental Figure S8. Principal component analysis (PCA) of normalized expression profiles for all expressed genes under LDs and SDs.

Supplemental Figure S9. DETs in each mutant (*mat-c.907* or *mat-c.943*) compared with the wild type (Bonus) under each photoperiod (LDs, SDs) at W1.0, W2.0 and W3.5.

Supplemental Table S1. *mat-c* (*hvcen*) mutants carrying different types of mutations in *HvCEN*.

Supplemental Table S2. Effects of amino acid substitutions in the *mat-c* (*hvcen*) mutants.

Supplemental Table S3. Normalized expression value (cpm), log2FC, FDR and annotation of all expressed transcripts.

Supplemental Table S4. Number of transcripts mutated in the two mutants compared to wild type.

Supplemental Table S5. GO enrichment analysis of photoperiod-independent DETs at W2.0.

Supplemental Table S6. Selected transcripts differentially regulated in the mutant MSA at W2.0 under LDs and SDs (FDR < 0.01).

Supplemental Table S7. GO enrichment analysis of photoperiodic-specific DETs (FDR < 0.01) at W3.5.

Supplemental Table S8. Selected photoperiod-independent/dependent DETs at W3.5 (FDR < 0.01).

Supplemental Table S9. Selected DETs involved in floral development and identity at W3.5 (FDR < 0.05).

Supplemental Table S10. Primers used in RT-qPCR and genotyping.

ACKNOWLEDGMENTS

We cordially thank Kerstin Luxa, Caren Dawidson, Thea Rütjes, and Andrea Lossow for excellent technical assistance and Artem Pankin for uploading the raw sequencing data to the European Nucleotide Archive.

Received November 20, 2018; accepted April 8, 2019; published April 19, 2019.

LITERATURE CITED

Abe M, Kobayashi Y, Yamamoto S, Daimon Y, Yamaguchi A, Ikeda Y, Ichinoki H, Notaguchi M, Goto K, Araki T (2005) FD, a bZIP protein mediating signals from the floral pathway integrator FT at the shoot apex. Science **309:** 1052–1056

Ahn JH, Miller D, Winter VJ, Banfield MJ, Lee JH, Yoo SY, Henz SR, Brady RL, Weigel D (2006) A divergent external loop confers antagonistic activity on floral regulators FT and TFL1. EMBO J **25:** 605–614

Alexa A, Rahnenführer J, Lengauer T (2006) Improved scoring of functional groups from gene expression data by decorrelating GO graph structure. Bioinformatics **22:** 1600–1607

Alqudah AM, Schnurbusch T (2014) Awn primordium to tipping is the most decisive developmental phase for spikelet survival in barley. Funct Plant Biol **41:** 424–436

Alvarez MA, Tranquilli G, Lewis S, Kippes N, Dubcovsky J (2016) Genetic and physical mapping of the earliness *per se* locus *Eps-A* ^{m} *1* in *Triticum monococcum* identifies *EARLY FLOWERING 3* (*ELF3*) as a candidate gene. Funct Integr Genomics **16:** 365–382

Arora R, Agarwal P, Ray S, Singh AK, Singh VP, Tyagi AK, Kapoor S (2007) MADS-box gene family in rice: Genome-wide identification, organization and expression profiling during reproductive development and stress. BMC Genomics **8:** 242

Bhavsar RB, Makley LN, Tsonis PA (2010) The other lives of ribosomal proteins. Hum Genomics **4:** 327–344

Boden SA, Cavanagh C, Cullis BR, Ramm K, Greenwood J, Jean Finnegan E, Trevaskis B, Swain SM (2015) Ppd-1 is a key regulator of inflorescence architecture and paired spikelet development in wheat. Nat Plants **1:** 14016

Bommert P, Whipple C (2018) Grass inflorescence architecture and meristem determinacy. Semin Cell Dev Biol **79:** 37–47

Bouveret R, Schönrock N, Gruissem W, Hennig L (2006) Regulation of flowering time by Arabidopsis MSI1. Development **133:** 1693–1702

Bradley D, Carpenter R, Copsey L, Vincent C, Rothstein S, Coen E (1996) Control of inflorescence architecture in Antirrhinum. Nature **379:** 791–797

Bradley D, Ratcliffe O, Vincent C, Carpenter R, Coen E (1997) Inflorescence commitment and architecture in Arabidopsis. Science **275:** 80–83

Bull H, Casao MC, Zwirek M, Flavell AJ, Thomas WTB, Guo W, Zhang R, Rapazote-Flores P, Kyriakidis S, Russell J, et al (2017) Barley SIX-ROWED SPIKE3 encodes a putative Jumonji C-type H3K9me2/me3 demethylase that represses lateral spikelet fertility. Nat Commun **8:** 936

Campoli C, von Korff M (2014) Genetic control of reproductive development in temperate cereals. *In* Fornara F, ed. Advances in botanical research. Elsevier, pp 131–158

Campoli C, Drosse B, Searle I, Coupland G, von Korff M (2012) Functional characterisation of HvCO1, the barley (*Hordeum vulgare*) flowering time ortholog of *CONSTANS*. Plant J **69:** 868–880

Casao MC, Karsai I, Igartua E, Gracia MP, Veisz O, Casas AM (2011) Adaptation of barley to mild winters: A role for PPDH2. BMC Plant Biol **11:** 164

Chanvivattana Y, Bishopp A, Schubert D, Stock C, Moon YH, Sung ZR, Goodrich J (2004) Interaction of Polycomb-group proteins controlling flowering in Arabidopsis. Development **131:** 5263–5276

Chen A, Dubcovsky J (2012) Wheat TILLING mutants show that the vernalization gene VRN1 down-regulates the flowering repressor VRN2 in leaves but is not essential for flowering. PLoS Genet **8:** e1003134

Chen H, Boutros PC (2011) VennDiagram: A package for the generation of highly-customizable Venn and Euler diagrams in R. BMC Bioinformatics **12:** 35

Choi Y, Sims GE, Murphy S, Miller JR, Chan AP (2012) Predicting the functional effect of amino acid substitutions and indels. PLoS One **7:** e46688

Coen ES, Meyerowitz EM (1991) The war of the whorls: Genetic interactions controlling flower development. Nature **353:** 31–37

Comadran J, Kilian B, Russell J, Ramsay L, Stein N, Ganal M, Shaw P, Bayer M, Thomas W, Marshall D, et al (2012) Natural variation in a homolog of Antirrhinum CENTRORADIALIS contributed to spring growth habit and environmental adaptation in cultivated barley. Nat Genet **44:** 1388–1392

Conesa A, Götz S, García-Gómez JM, Terol J, Talón M, Robles M (2005) Blast2GO: A universal tool for annotation, visualization and analysis in functional genomics research. Bioinformatics **21:** 3674–3676

Conti L, Bradley D (2007) TERMINAL FLOWER1 is a mobile signal controlling Arabidopsis architecture. Plant Cell **19:** 767–778

Corbesier L, Vincent C, Jang S, Fornara F, Fan Q, Searle I, Giakountis A, Farrona S, Gissot L, Turnbull C, Coupland G (2007) FT protein movement contributes to long-distance signaling in floral induction of Arabidopsis. Science **316:** 1030–1033

Danilevskaya ON, Meng X, Hou Z, Ananiev EV, Simmons CR (2008) A genomic and expression compendium of the expanded PEBP gene family from maize. Plant Physiol **146:** 250–264

Danilevskaya ON, Meng X, Ananiev EV (2010) Concerted modification of flowering time and inflorescence architecture by ectopic expression of TFL1-like genes in maize. Plant Physiol **153:** 238–251

Deng X, Gu L, Liu C, Lu T, Lu F, Lu Z, Cui P, Pei Y, Wang B, Hu S, et al (2010) Arginine methylation mediated by the Arabidopsis homolog of PRMT5 is essential for proper pre-mRNA splicing. Proc Natl Acad Sci USA **107:** 19114–19119

Derkacheva M, Steinbach Y, Wildhaber T, Mozgová I, Mahrez W, Nanni P, Bischof S, Gruissem W, Hennig L (2013) Arabidopsis MSI1 connects LHP1 to PRC2 complexes. EMBO J **32:** 2073–2085

Digel B, Pankin A, von Korff M (2015) Global transcriptome profiling of developing leaf and shoot apices reveals distinct genetic and environmental control of floral transition and inflorescence development in barley. Plant Cell **27:** 2318–2334

Digel B, Tavakol E, Verderio G, Tondelli A, Xu X, Cattivelli L, Rossini L, von Korff M (2016) Photoperiod1 (Ppd-H1) controls leaf size. Plant Physiol **172:** 405–415

Dixon LE, Farré A, Finnegan EJ, Orford S, Griffiths S, Boden SA (2018) Developmental responses of bread wheat to changes in ambient temperature following deletion of a locus that includes FLOWERING LOCUS T1. Plant Cell Environ **41:** 1715–1725

Druka A, Franckowiak J, Lundqvist U, Bonar N, Alexander J, Houston K, Radovic S, Shahinnia F, Vendramin V, Morgante M, et al (2011) Genetic dissection of barley morphology and development. Plant Physiol **155:** 617–627

Ejaz M, von Korff M (2017) The genetic control of reproductive development under high ambient temperature. Plant Physiol **173:** 294–306

Faure S, Turner AS, Gruszka D, Christodoulou V, Davis SJ, von Korff M, Laurie DA (2012) Mutation at the circadian clock gene *EARLY MATURITY 8* adapts domesticated barley (*Hordeum vulgare*) to short growing seasons. Proc Natl Acad Sci USA **109:** 8328–8333

Franckowiak JD, Lundqvist U (2011) Descriptions of barley genetic stocks for 2011. Barley Genet Newsl **41:** 11–53

Gao X, Liang W, Yin C, Ji S, Wang H, Su X, Guo C, Kong H, Xue H, Zhang D (2010) The SEPALLATA-like gene OsMADS34 is required for rice inflorescence and spikelet development. Plant Physiol **153:** 728–740

Ghiglione HO, Gonzalez FG, Serrago R, Maldonado SB, Chilcott C, Curá JA, Miralles DJ, Zhu T, Casal JJ (2008) Autophagy regulated by day length determines the number of fertile florets in wheat. Plant J **55:** 1010–1024

Halliwell J, Borrill P, Gordon A, Kowalczyk R, Pagano ML, Saccomanno B, Bentley AR, Uauy C, Cockram J (2016) Systematic Investigation of FLOWERING LOCUS T-like poaceae gene families identifies the short-day expressed flowering pathway gene, TaFT3 in wheat (*Triticum aestivum* L.). Front Plant Sci **7:** 857

Hanano S, Goto K (2011) Arabidopsis TERMINAL FLOWER1 is involved in the regulation of flowering time and inflorescence development through transcriptional repression. Plant Cell **23:** 3172–3184

Hemming MN, Peacock WJ, Dennis ES, Trevaskis B (2008) Low-temperature and daylength cues are integrated to regulate FLOWERING LOCUS T in barley. Plant Physiol **147:** 355–366

Hennig L, Bouveret R, Gruissem W (2005) MSI1-like proteins: An escort service for chromatin assembly and remodeling complexes. Trends Cell Biol **15:** 295–302

Hicks KA, Millar AJ, Carré IA, Somers DE, Straume M, Meeks-Wagner DR, Kay SA (1996) Conditional circadian dysfunction of the Arabidopsis early-flowering 3 mutant. Science **274:** 790–792

Ho WW, Weigel D (2014) Structural features determining flower-promoting activity of Arabidopsis FLOWERING LOCUS T. Plant Cell **26:** 552–564

Ikeda K, Ito M, Nagasawa N, Kyozuka J, Nagato Y (2007) Rice ABERRANT PANICLE ORGANIZATION 1, encoding an F-box protein, regulates meristem fate. Plant J **51:** 1030–1040

Ito T, Kim GT, Shinozaki K (2000) Disruption of an Arabidopsis cytoplasmic ribosomal protein S13-homologous gene by transposon-mediated mutagenesis causes aberrant growth and development. Plant J **22:** 257–264

Jacob Y, Feng S, LeBlanc CA, Bernatavichute YV, Stroud H, Cokus S, Johnson LM, Pellegrini M, Jacobsen SE, Michaels SD (2009) ATXR5 and ATXR6 are H3K27 monomethyltransferases required for chromatin structure and gene silencing. Nat Struct Mol Biol **16:** 763–768

Jaeger KE, Pullen N, Lamzin S, Morris RJ, Wigge PA (2013) Interlocking feedback loops govern the dynamic behavior of the floral transition in Arabidopsis. Plant Cell **25:** 820–833

Jensen CS, Salchert K, Nielsen KK (2001) A TERMINAL FLOWER1-like gene from perennial ryegrass involved in floral transition and axillary meristem identity. Plant Physiol **125:** 1517–1528

Jeon Y, Park YJ, Cho HK, Jung HJ, Ahn TK, Kang H, Pai HS (2015) The nucleolar GTPase nucleostemin-like 1 plays a role in plant growth and senescence by modulating ribosome biogenesis. J Exp Bot **66:** 6297–6310

Jiang K, Liberatore KL, Park SJ, Alvarez JP, Lippman ZB (2013) Tomato yield heterosis is triggered by a dosage sensitivity of the florigen pathway that fine-tunes shoot architecture. PLoS Genet **9:** e1004043

Kaneko-Suzuki M, Kurihara-Ishikawa R, Okushita-Terakawa C, Kojima C, Nagano-Fujiwara M, Ohki I, Tsuji H, Shimamoto K, Taoka KI (2018) TFL1-like proteins in rice antagonize rice FT-like protein in inflorescence development by competition for complex formation with 14-3-3 and FD. Plant Cell Physiol **59:** 458–468

Kardailsky I, Shukla VK, Ahn JH, Dagenais N, Christensen SK, Nguyen JT, Chory J, Harrison MJ, Weigel D (1999) Activation tagging of the floral inducer FT. Science **286:** 1962–1965

Kernich GC, Halloran GM, Flood RG (1997) Variation in duration of pre-anthesis phases of development in barley (*Hordeum vulgare*). Aust J Agric Res **48:** 59–66

Kirby EJM, Appleyard M (1987) Development and structure of the wheat plant. *In* Lupton FGH, ed. Wheat breeding. Springer, pp 287–311

Kobayashi K, Maekawa M, Miyao A, Hirochika H, Kyozuka J (2010) PANICLE PHYTOMER2 (PAP2), encoding a SEPALLATA subfamily MADS-box protein, positively controls spikelet meristem identity in rice. Plant Cell Physiol **51:** 47–57

Kobayashi Y, Kaya H, Goto K, Iwabuchi M, Araki T (1999) A pair of related genes with antagonistic roles in mediating flowering signals. Science **286:** 1960–1962

Komatsuda T, Pourkheirandish M, He C, Azhaguvel P, Kanamori H, Perovic D, Stein N, Graner A, Wicker T, Tagiri A, et al (2007) Six-rowed barley originated from a mutation in a homeodomain-leucine zipper I-class homeobox gene. Proc Natl Acad Sci USA **104:** 1424–1429

Komiya R, Ikegami A, Tamaki S, Yokoi S, Shimamoto K (2008) Hd3a and RFT1 are essential for flowering in rice. Development **135:** 767–774

Koppolu R, Anwar N, Sakuma S, Tagiri A, Lundqvist U, Pourkheirandish M, Rutten T, Seiler C, Himmelbach A, Ariyadasa R, et al (2013) Six-rowed spike4 (Vrs4) controls spikelet determinacy and row-type in barley. Proc Natl Acad Sci USA **110:** 13198–13203

Krieger U, Lippman ZB, Zamir D (2010) The flowering gene SINGLE FLOWER TRUSS drives heterosis for yield in tomato. Nat Genet **42:** 459–463

Li H (2013) Aligning sequence reads, clone sequences and assembly contigs with BWA-MEM. arXiv: 1303.3997

Li H, Handsaker B, Wysoker A, Fennell T, Ruan J, Homer N, Marth G, Abecasis G, Durbin R; 1000 Genome Project Data Processing Subgroup (2009) The Sequence alignment/map (SAM) format and SAMtools. Bioinformatics **25:** 2078–2079

Lifschitz E, Ayre BG, Eshed Y (2014) Florigen and anti-florigen---a systemic mechanism for coordinating growth and termination in flowering plants. Front Plant Sci **5:** 465

Liu XL, Covington MF, Fankhauser C, Chory J, Wagner DR (2001) ELF3 encodes a circadian clock-regulated nuclear protein that functions in an Arabidopsis PHYB signal transduction pathway. Plant Cell **13:** 1293–1304

Lundqvist U (2014) Scandinavian mutation research in barley - a historical review. Hereditas **151:** 123–131

Malcomber ST, Kellogg EA (2005) *SEPALLATA* gene diversification: brave new whorls. Trends Plant Sci **10:** 427–435

Mascher M, Gundlach H, Himmelbach A, Beier S, Twardziok SO, Wicker T, Radchuk V, Dockter C, Hedley PE, Russell J, et al (2017) A chromosome conformation capture ordered sequence of the barley genome. Nature **544:** 427–433

Matyszczak I (2014). Characterization of early maturity barley mutants praematurum-a, -b and –c. PhD. thesis. Aarhus University, Department of Molecular Biology and Genetics, Faculty of Science and Technology, Aarhus, Denmark.

McGarry RC, Ayre BG (2012) Manipulating plant architecture with members of the CETS gene family. Plant Sci **188-189:** 71–81

McKenna A, Hanna M, Banks E, Sivachenko A, Cibulskis K, Kernytsky A, Garimella K, Altshuler D, Gabriel S, Daly M, et al (2010) The Genome Analysis Toolkit: A MapReduce framework for analyzing next-generation DNA sequencing data. Genome Res **20:** 1297–1303

Mulki MA, Bi X, von Korff M (2018) FLOWERING LOCUS T3 controls spikelet initiation but not floral development. Plant Physiol **178:** 1170–1186

Nakagawa M, Shimamoto K, Kyozuka J (2002) Overexpression of RCN1 and RCN2, rice TERMINAL FLOWER 1/CENTRORADIALIS homologs, confers delay of phase transition and altered panicle morphology in rice. Plant J **29:** 743–750

Naora H (1999) Involvement of ribosomal proteins in regulating cell growth and apoptosis: Translational modulation or recruitment for extraribosomal activity? Immunol Cell Biol **77:** 197–205

Niu L, Lu F, Pei Y, Liu C, Cao X (2007) Regulation of flowering time by the protein arginine methyltransferase AtPRMT10. EMBO Rep **8:** 1190–1195

Ohshima S, Murata M, Sakamoto W, Ogura Y, Motoyoshi F (1997) Cloning and molecular analysis of the Arabidopsis gene *Terminal Flower 1*. Mol Gen Genet **254:** 186–194

Park SJ, Jiang K, Tal L, Yichie Y, Gar O, Zamir D, Eshed Y, Lippman ZB (2014) Optimization of crop productivity in tomato using induced mutations in the florigen pathway. Nat Genet **46:** 1337–1342

Patro R, Duggal G, Love MI, Irizarry RA, Kingsford C (2017) Salmon provides fast and bias-aware quantification of transcript expression. Nat Methods **14:** 417–419

Pearce S, Vanzetti LS, Dubcovsky J (2013) Exogenous gibberellins induce wheat spike development under short days only in the presence of VERNALIZATION1. Plant Physiol **163:** 1433–1445

Pei Y, Niu L, Lu F, Liu C, Zhai J, Kong X, Cao X (2007) Mutations in the Type II protein arginine methyltransferase AtPRMT5 result in pleiotropic developmental defects in Arabidopsis. Plant Physiol **144:** 1913–1923

Pinon V, Etchells JP, Rossignol P, Collier SA, Arroyo JM, Martienssen RA, Byrne ME (2008) Three PIGGYBACK genes that specifically influence leaf patterning encode ribosomal proteins. Development **135:** 1315–1324

Preibisch S, Saalfeld S, Tomancak P (2009) Globally optimal stitching of tiled 3D microscopic image acquisitions. Bioinformatics **25:** 1463–1465

Ramsay L, Comadran J, Druka A, Marshall DF, Thomas WT, Macaulay M, MacKenzie K, Simpson C, Fuller J, Bonar N, et al (2011) INTERMEDIUM-C, a modifier of lateral spikelet fertility in barley, is an ortholog of the maize domestication gene TEOSINTE BRANCHED 1. Nat Genet **43:** 169–172

Riggs TJ, Kirby EJM (1978) Developmental consequences of two-row and six-row ear type in spring barley: 1. Genetical analysis and comparison of mature plant characters. J Agric Sci **91:** 199–205

Ritchie ME, Phipson B, Wu D, Hu Y, Law CW, Shi W, Smyth GK (2015) limma powers differential expression analyses for RNA-sequencing and microarray studies. Nucleic Acids Res **43:** e47

Ruiz-García L, Madueño F, Wilkinson M, Haughn G, Salinas J, Martínez-Zapater JM (1997) Different roles of flowering-time genes in the activation of floral initiation genes in Arabidopsis. Plant Cell **9:** 1921–1934

Ryu MY, Cho SK, Kim WT (2009) RNAi suppression of RPN12a decreases the expression of type-A ARRs, negative regulators of cytokinin signaling pathway, in Arabidopsis. Mol Cells **28:** 375–382

Sasani S, Hemming MN, Oliver SN, Greenup A, Tavakkol-Afshari R, Mahfoozi S, Poustini K, Sharifi HR, Dennis ES, Peacock WJ, Trevaskis B (2009) The influence of vernalization and daylength on expression of flowering-time genes in the shoot apex and leaves of barley (*Hordeum vulgare*). J Exp Bot **60:** 2169–2178

Schaller GE, Street IH, Kieber JJ (2014) Cytokinin and the cell cycle. Curr Opin Plant Biol **21:** 7–15

Schindelin J, Arganda-Carreras I, Frise E, Kaynig V, Longair M, Pietzsch T, Preibisch S, Rueden C, Saalfeld S, Schmid B, et al (2012) Fiji: An open-source platform for biological-image analysis. Nat Methods **9:** 676–682

Schmitz J, Franzen R, Ngyuen TH, Garcia-Maroto F, Pozzi C, Salamini F, Rohde W (2000) Cloning, mapping and expression analysis of barley MADS-box genes. Plant Mol Biol **42:** 899–913

Schmitz RJ, Sung S, Amasino RM (2008) Histone arginine methylation is required for vernalization-induced epigenetic silencing of FLC in winter-annual Arabidopsis thaliana. Proc Natl Acad Sci USA **105:** 411–416

Shannon S, Meeks-Wagner DR (1991) A mutation in the Arabidopsis TFL1 gene affects inflorescence meristem development. Plant Cell **3:** 877–892

Steinbach Y, Hennig L (2014) Arabidopsis MSI1 functions in photoperiodic flowering time control. Front Plant Sci **5:** 77

Supek F, Bošnjak M, Škunca N, Šmuc T (2011) REVIGO summarizes and visualizes long lists of gene ontology terms. PLoS One **6:** e21800

Tamaki S, Matsuo S, Wong HL, Yokoi S, Shimamoto K (2007) Hd3a protein is a mobile flowering signal in rice. Science **316:** 1033–1036

Taoka K, Ohki I, Tsuji H, Furuita K, Hayashi K, Yanase T, Yamaguchi M, Nakashima C, Purwestri YA, Tamaki S, et al (2011) 14-3-3 Proteins act as intracellular receptors for rice Hd3a florigen. Nature **476:** 332–335

Teichmann T, Muhr M (2015) Shaping plant architecture. Front Plant Sci **6:** 233

Theissen G (2001) Development of floral organ identity: Stories from the MADS house. Curr Opin Plant Biol **4:** 75–85

Turck F, Fornara F, Coupland G (2008) Regulation and identity of florigen: FLOWERING LOCUS T moves center stage. Annu Rev Plant Biol **59:** 573–594

Turnbull CGN (2005) Plant Architecture and Its Manipulation. John Wiley & Sons, Hoboken, NJ

van Esse GW, Walla A, Finke A, Koornneef M, Pecinka A, von Korff M (2017) Six-rowed Spike3 (VRS3) is a histone demethylase that controls lateral spikelet development in barley. Plant Physiol **174:** 2397–2408

Waddington SR, Cartwright PM, Wall PC (1983) A quantitative scale of spike initial and pistil development in barley and wheat. Ann Bot **51:** 119–130

Wang X, Zhang Y, Ma Q, Zhang Z, Xue Y, Bao S, Chong K (2007) SKB1-mediated symmetric dimethylation of histone H4R3 controls flowering time in Arabidopsis. EMBO J **26:** 1934–1941

Wang X, Gingrich DK, Deng Y, Hong Z (2012) A nucleostemin-like GTPase required for normal apical and floral meristem development in Arabidopsis. Mol Biol Cell **23:** 1446–1456

Wigge PA, Kim MC, Jaeger KE, Busch W, Schmid M, Lohmann JU, Weigel D (2005) Integration of spatial and temporal information during floral induction in Arabidopsis. Science **309:** 1056–1059

Yan L, Fu D, Li C, Blechl A, Tranquilli G, Bonafede M, Sanchez A, Valarik M, Yasuda S, Dubcovsky J (2006) The wheat and barley vernalization gene VRN3 is an orthologue of FT. Proc Natl Acad Sci USA **103:** 19581–19586

Yeung K, Seitz T, Li S, Janosch P, McFerran B, Kaiser C, Fee F, Katsanakis KD, Rose DW, Mischak H, Sedivy JM, Kolch W (1999) Suppression of Raf-1 kinase activity and MAP kinase signalling by RKIP. Nature **401:** 173–177

Youssef HM, Eggert K, Koppolu R, Alqudah AM, Poursarebani N, Fazeli A, Sakuma S, Tagiri A, Rutten T, Govind G, et al (2017) VRS2 regulates hormone-mediated inflorescence patterning in barley. Nat Genet **49:** 157–161

Zagotta MT, Hicks KA, Jacobs CI, Young JC, Hangarter RP, Meeks-Wagner DR (1996) The Arabidopsis ELF3 gene regulates vegetative photomorphogenesis and the photoperiodic induction of flowering. Plant J **10:** 691–702

Zahn LM, Kong H, Leebens-Mack JH, Kim S, Soltis PS, Landherr LL, Soltis DE, Depamphilis CW, Ma H (2005) The evolution of the *SEPALLATA* subfamily of MADS-box genes: A preangiosperm origin with multiple duplications throughout angiosperm history. Genetics **169:** 2209–2223